SIAM J. APPL. MATH.
Vol. 61, No. 5, pp. 1762–1801
© 2001 Society for Industrial and Applied Mathematics

SYNCHRONIZATION AND TRANSIENT DYNAMICS IN THE CHAINS OF ELECTRICALLY COUPLED FITZHUGH–NAGUMO OSCILLATORS*

GEORGI S. MEDVEDEV† AND NANCY KOPELL‡

Abstract. Chains of N FitzHugh–Nagumo oscillators with a gradient in natural frequencies and strong diffusive coupling are analyzed in this paper. We study the system's dynamics in the limit of infinitely large coupling and then treat the case when the coupling is large but finite as a perturbation of the former case. In the large coupling limit, the $2N$-dimensional phase space has an unexpected structure: there is an $(N-1)$-dimensional cylinder foliated by periodic orbits with an integral that is constant on each orbit. When the coupling is large but finite, this cylinder becomes an analog of an inertial manifold. The phase trajectories approach the cylinder on the fast time scale and then slowly drift along it toward a unique limit cycle. We analyze these dynamics using geometric theory for singularly perturbed dynamical systems, asymptotic expansions of solutions (rigorously justified), and Lyapunov's method.

Key words. compartmental model, chains of coupled oscillators, synchronization, singularly perturbed systems, Lyapunov's method

AMS subject classifications. 34E20, 34D23, 92C20

PII. S0036139900368807

1. Introduction.

Spatially distributed neurons are often modeled as a collection of compartments [11, 16], with connections between adjacent compartments represented as simple electrotonic coupling. It is known that having different distribution of ionic currents in the different compartments or different geometry in the compartments can affect the behavioral repertoire of the cells (e.g., [21, 15] and references therein).

This paper is motivated by recent work of C. Wilson and J. Callaway on firing patterns in dopamine-releasing neurons [30]. In work aimed at understanding the origin of bursting patterns in vivo, Wilson and Callaway used calcium imaging, electrophysiology, and modeling to investigate patterns of firing in an in vitro preparation containing these cells. Their experimental data suggest that a single such cell may be thought of as a chain of oscillating compartments, with differences in natural frequencies along the chain created by differences in calcium dynamics. The minimal model introduced to describe some features of their observations is a Morris–Lecar-like set of equations [18] for the electrical potential v and the Ca-concentration u in each compartment:

$$\text{C}\frac{dv}{dt} = g_{Ca}(v)(E_{Ca}-v) + \left(g_K(v)+g_{KCa}(u)\right)(E_K-v) + g_{leak}(E_l-v), \tag{1.1}$$

*Received by the editors March 6, 2000; accepted for publication (in revised form) October 18, 2000; published electronically March 7, 2001.
http://www.siam.org/journals/siap/61-5/36880.html

†Program in Applied and Computational Mathematics, Princeton University, Princeton, NJ 08544-1000, and School of Mathematics, Institute for Advanced Study, Einstein Drive, Princeton, NJ 08540 (medvedev@math.princeton.edu). The work of this author was partially supported by NSF VIGRE grant DMS-9810783 and NSF grant DMS-9729992.

‡Department of Mathematics, Boston University, 111 Cummington Street, Boston, MA 02215 (nk@math.bu.edu). The work of this author was partially supported by NSF grant DMS-9706694 and NIH grant MH47150.

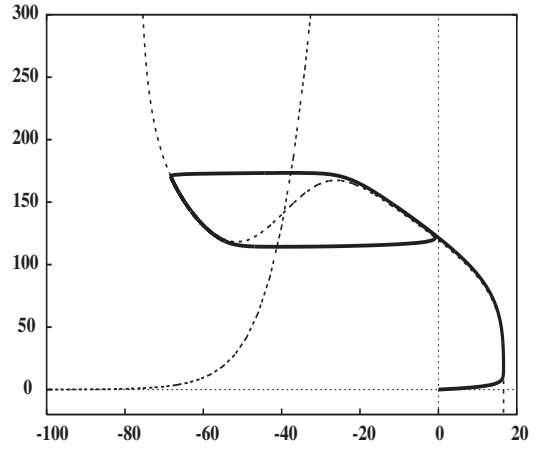

FIG. 1. *The $v-u$ phase plane for a relaxation oscillator* (1.1). *The dotted curves are the v-nullcline (cubic shaped) and the u-nullcline. The membrane potential, v, is measured in the units of mV and the calcium concentration, u, is in the units of nM, as in the model in* [30]. *The bold curve is a phase trajectory of* (1.1) *approaching the limit cycle.*

$$\frac{du}{dt} = \omega \left(\frac{g_{Ca}(v)(E_{Ca} - v)}{\tau} - \frac{u}{\tau_{Ca}} \right),$$

where C is the membrane capacitance, τ^{-1} relates voltage change due to Ca input to the change in the Ca concentration, and the factor ω varies along the chain. The model is derived as a discrete cable equation [11], using a small number of nonlinear conductances. $g_{Ca}(v)$ and $g_K(v)$ are voltage dependent calcium and potassium conductances and $g_{KCa}(u)$ is a calcium dependent potassium conductance; there is also a small leak conductance g_{leak} and a slow calcium removal with time constant τ_{Ca}^{-1}. More information is in [30]. In the range of parameters of interest, (1.1) is a relaxation oscillator (Figure 1). The compartments are coupled through the voltage variables by terms in the first equation in (1.1) of the form $d\left(r_i(v_{i+1} - v_i) + r_{i-1}(v_{i-1} - v_i)\right)$, where $d \gg 1$ is the strength of the coupling and $r_i > 0$.

In the current paper, we study a related set of equations to understand some dynamical features observed in both the experiments and the model (1.1). The essential features are as follows:

1. Though the compartments have significantly different natural frequencies, the voltages in all compartments are essentially identical (Figure 2(a)).

2. The u variables (calcium concentration in the experiments) have different amplitudes but the same time courses.

3. The u variables approach a steady-state oscillation via a long transition period. During this period, the amplitudes of the oscillations in the compartments with the low natural frequencies increase, and those of compartments with high natural frequencies decrease; the time courses remain the same during the transition (Figure 2(b)). The model has long transients even for strong coupling (large d).

To understand the origin of the long transition and its dependence on coupling strength, we consider a set of equations that exhibit qualitatively the same dynamics as (1.1), but which are more amenable to analysis. We use the coupled FitzHugh–

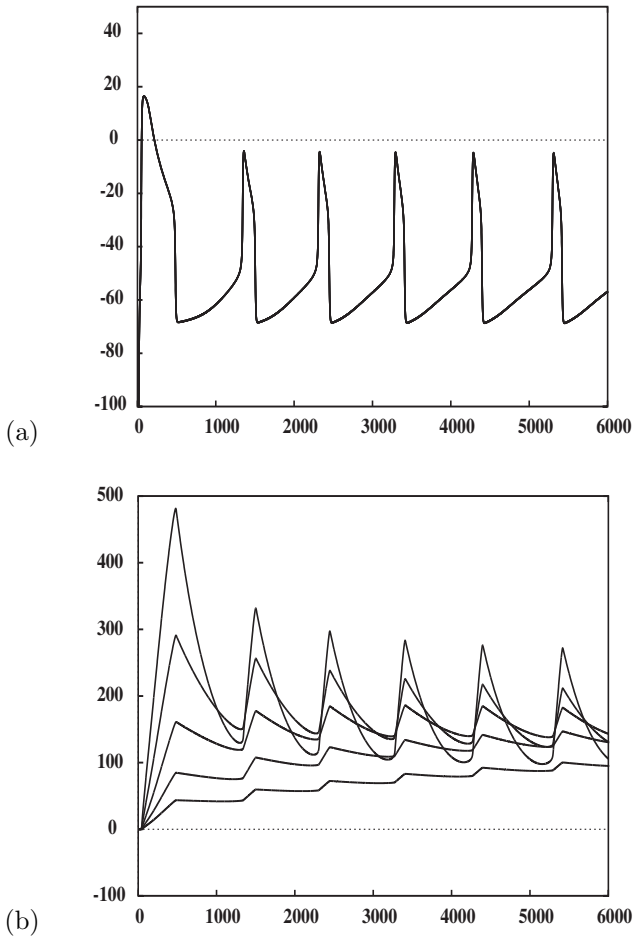

FIG. 2. *The time series plots of* (a) *the voltage variables,* v_i*, and* (b) *the concentration variables,* u_i*, of the chain of five relaxation oscillators* (1.1) *strongly coupled through fast variables,* v_i*. The time unit is ms. For the values of parameters, see* [30]*. Note that the voltage variables are almost identical. The amplitudes of the concentration variables gradually change, but everything stays in synchrony.*

Nagumo equations

$$
\begin{aligned}
\epsilon\frac{dv_1}{dt} &= f(v_1) - u_1 + d(v_2 - v_1),\\
\epsilon\frac{dv_i}{dt} &= f(v_i) - u_i + d(v_{i+1} - 2v_i + v_{i-1}), \quad i = 2, 3, \ldots, N-1,\\
\epsilon\frac{dv_N}{dt} &= f(v_N) - u_N - d(v_N - v_{N-1}),\\
\frac{du_i}{dt} &= \omega_i v_i, \quad i = 1, 2, \ldots, N,
\end{aligned}
\tag{1.2}
$$

where ω_i's are different natural frequencies of the individual oscillators, $d \gg 1$, $0 < \epsilon \ll 1$, and the potential f has a qualitative "cubic" form. The coupling terms have the form of a discrete Laplace operator, like the original model of Wilson and Callaway

[30], without the gradient in coupling strengths of the original model. In section 6, we show how to modify our analysis to cover chains with inhomogeneous coupling (see Remark 6.1). In the limit of strong coupling ($d \to \infty$), we find that system (1.2) has an unexpected mathematical structure: a family of periodic orbits, which form an attracting $(N-1)$-dimensional cylinder in $2N$-dimensional phase space. For infinite coupling, a phase trajectory approaches one of these periodic orbits determined by the initial condition. When the coupling is large but finite the phase trajectory approaches the cylinder of periodic orbits and then drifts along it slowly with rate $O(\frac{1}{d})$ toward a unique limit cycle of the coupled system. This drift corresponds to the transient dynamics clearly seen from the both numerics and experiments. Therefore, the transients are longer for strong coupling.

Our analysis uses ideas from the geometric theory of singularly perturbed dynamical systems [14]. To understand the dynamics of (1.2), one has to find the slow manifolds associated with (1.2). However, even for a system of two coupled oscillators of type (1.2) the slow manifolds and their boundaries are not evident. A crucial observation is that

$$v_{i+1} - v_i = O(\delta), \quad \delta \equiv \frac{1}{d}, \quad i = 1, 2, \ldots, N-1. \tag{1.3}$$

This scaling is plausible from the form of the v-equations in (1.2) and is rigorously justified later in the paper. It follows from (1.3) that the coupling terms $d(v_{i+1} - v_i) = O(1)$. Since all of the v-components are equal to leading order, the coupling terms on the parts of trajectories can be parametrized just by the first v-component, v_1:

$$c_i(v_1) \equiv d(v_{i+1} - v_i). \tag{1.4}$$

The ansatz (1.4) and (1.3) can be used to uncouple (1.2), making the analysis possible. However, the functions $c_i(v_1)$ are not known a priori. Much of the work is to show the sense in which the c_i are well defined and to calculate them. Indeed, when the coupling is finite (but large), the $c_i(v_1)$ change from cycle to cycle, and the size of this change is closely related, inversely, to the length of the transient behavior.

The paper is organized as follows. We start in section 2 with some background information about single relaxation oscillators and a formulation of the problem for two oscillators, using simulations to motivate an appropriate notion of synchrony. In section 3 we show heuristically how to compute the functions $c(v_1) = d(v_2 - v_1)$ and discuss the geometry of the fast and slow manifolds of the equations associated with this calculation. Using the heuristic calculation of $c(v_1)$, we can then do a formal construction of the synchronous solutions to the coupled equations. The calculations use an asymptotic analysis in powers of δ. At lowest order, we obtain a description of the slow manifolds and the frequency of the coupled system. We also obtain an integral for the coupled system, defined on a two-dimensional submanifold foliated by periodic solutions. At the next order in δ, we see that there is a drift in this function, which is no longer an integral. A direct computation of the drift shows that the transient part of the trajectory tends toward a unique periodic solution of the infinite coupling equations. This computation is done with estimates in a general setting, and explicitly for an example.

The direct asymptotic calculation is too cumbersome to be easily used for a chain of oscillators. Hence, in section 5, a different approach is developed, using a Lyapunov function inspired by the asymptotics. The analysis from this Lyapunov function recovers the $O(\delta)$ analysis from section 3 in a more conceptual and algebraically easier

manner. Using this new tool, the behavior of the chain of N oscillators is analyzed in section 6. We show that, for $\delta = 0$, there is an $(N-1)$-dimensional manifold foliated by periodic solutions, and the system quickly (time $O(\epsilon)$) approaches this manifold. As for the $N = 2$ case, when $\delta > 0$ there is a Lyapunov function, and trajectories approach a unique periodic orbit of the $\delta = 0$ equations.

All of the above analysis depended on the use of the ansatz (1.3). In section 7, we give a rigorous justification of the previous formal asymptotic results. In particular, we prove that any trajectory of (1.2) with initial data from a bounded domain of the phase space will converge to a unique limit cycle after a transition period of time $O(d)$.

In section 8, we show the surprising result that the conclusions of the paper need not hold after subtle changes in the form of the nullcline of the slow variable, even though such changes do not affect the behavior of the uncoupled oscillator. More specifically, we modify the u equations of (1.2) to

$$\frac{du_i}{dt} = \omega_i(v_i - \kappa u_i)$$

and show that the dynamics can be very sensitive to the value of κ. We explain the origin of this effect and discuss the relationship of this effect to the behavior of the motivating example (1.1).

2. Formulation of the problem. In the present section we formulate the problem for a system of two FitzHugh–Nagumo oscillators coupled diffusively:

$$\begin{aligned} \epsilon\frac{dv_i}{dt} &= f(v_i) - u_i + d(v_j - v_i), \quad i = 1, 2, \quad j = 3 - i, \\ \frac{du_i}{dt} &= \omega_i v_i, \end{aligned} \tag{2.1}$$

where $0 < \epsilon \ll 1$ and $d > 0$. In analogy to the physiological model (1.1), functions v_i and u_i in these equations represent voltage and concentration variables, respectively. A piecewise smooth function $f(v)$ is assumed to have a qualitatively cubic shape, e.g., $f(x) = x(1 - x^2)$. Henceforth for definiteness we will assume $\omega_1 < \omega_2$.

The numerical simulations of (2.1) suggest that when the coupling is sufficiently strong ($d \gg 1$) the system possesses a phase-synchronous solution even though the natural frequencies ω_1 and ω_2 are very different. The time series plotted in Figure 3(a) show that $v_1(t)$ and $v_2(t)$ undergo almost identical oscillations with a small phase shift. After some transition period, the concentration variables u_1 and u_2 exhibit synchronous oscillations in phase, but these oscillations have different amplitudes. During the transition period preceding the steady state oscillations, the amplitude of u_1 gradually increases while that of u_2 decreases but both variables stay in synchrony (see Figure 3(b)).

Before embarking upon an analysis of phase space trajectories of the coupled system of (2.1), we briefly recall some facts and terminology from the theory developed for a single relaxation oscillator:

$$\begin{aligned} \epsilon\frac{dv}{dt} &= f(v) - u, \\ \frac{du}{dt} &= \omega v. \end{aligned} \tag{2.2}$$

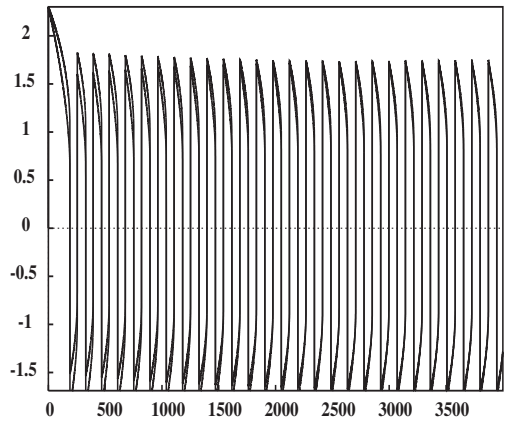

(a)

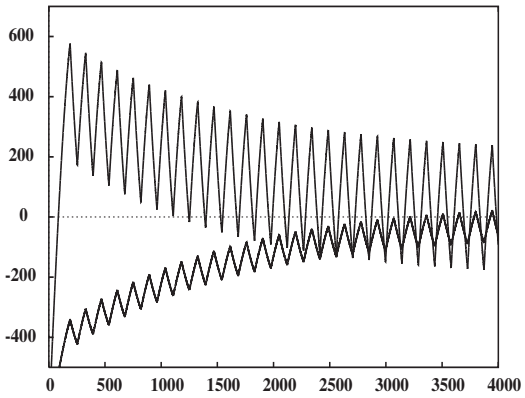

(b)

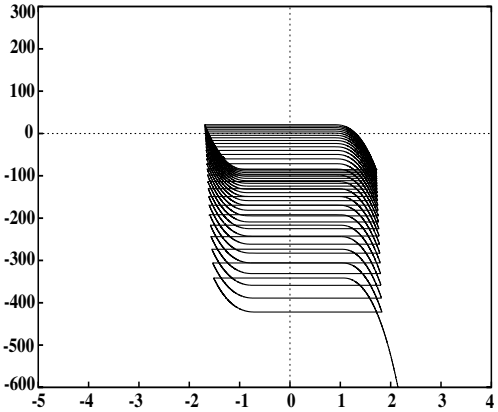

(c)

FIG. 3. *The time series plots for* (a) *the voltage variables,* $v_1(t)$ *and* $v_2(t)$*, and* (b) *the concentration variables* $u_1(t)$ *and* $u_2(t)$ *of a system of two coupled oscillators* (2.1)*. The values of parameters are* $d = 1000$*,* $\omega_1 = 1$*,* $\omega_2 = 4$*, and* $f(x) = 100x(1.5-x)(1.5+x)$*. Note that the variables* v_i *and* u_i *exhibit the dynamics similar to those of the corresponding variables of the chain of coupled oscillators of type* (1.1) *shown in Figure* 2*. The phase trajectory* $(v_1(t), u_1(t))$ *of the first oscillator is given in* (c)*. The trajectory slowly approaches from below the limit cycle. The slow evolution takes place along the family of periodic orbits of the* $O(1)$ *system.*

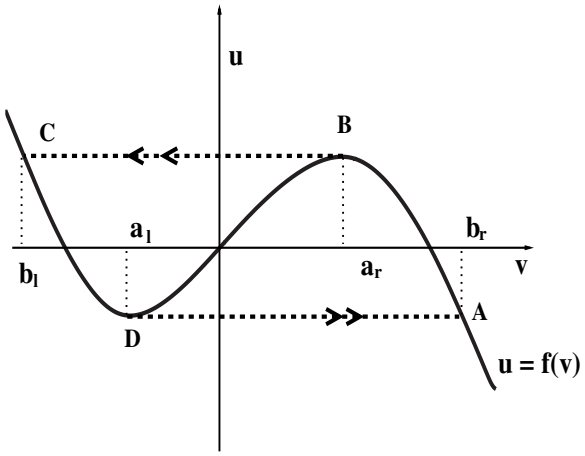

FIG. 4. *The $v-u$ phase plane for a relaxation oscillator* (2.2). *The u-nullcline coincides with the u-axis. The bold cubic shaped curve represents the v-nullcline. The directed segments BC and DA denote the fast parts of the system's trajectory, and the branches CD and AB of the cubic parabola denote the slow manifolds.*

The system (2.2) can be reformulated with a change of the time variable $\tau = \frac{t}{\epsilon}$:

$$\begin{aligned} \frac{dv}{d\tau} &= f(v) - u, \\ \frac{du}{d\tau} &= \epsilon\omega v. \end{aligned} \tag{2.3}$$

The time scale given by τ is said to be *fast* whereas that for t is *slow*. Thus, we call (2.2) the slow system and (2.3) the fast system. There are two limiting equations, one naturally associated with each scaling as $\epsilon \to 0$. Letting $\epsilon \to 0$ in (2.3), we obtain the system

$$\begin{aligned} \frac{dv}{d\tau} &= f(v) - u, \\ \frac{du}{d\tau} &= 0. \end{aligned} \tag{2.4}$$

According to the equation (2.4) for the reduced fast system the variable v, referred to as a fast variable, will vary while u will remain constant. On the other hand, if we let $\epsilon \to 0$ in (2.2), the limiting equations are

$$\begin{aligned} u &= f(v), \\ \frac{du}{dt} &= \omega v. \end{aligned} \tag{2.5}$$

The reduced slow system (2.5) defines a differential flow on the manifold $\Gamma = \{(u, v) : u = f(v)\}$ given by the first equation.

A singular solution of (2.2) is constructed by piecing together the solutions of reduced fast and slow systems (2.3) and (2.4), respectively. The resulting phase trajectory Z_0, corresponding to the stable limit cycle, is given in Figure 4. It consists of the slow segments $\overrightarrow{AB}$ and $\overrightarrow{CD}$ connected by the instantaneous jumps $\overrightarrow{BC}$ and

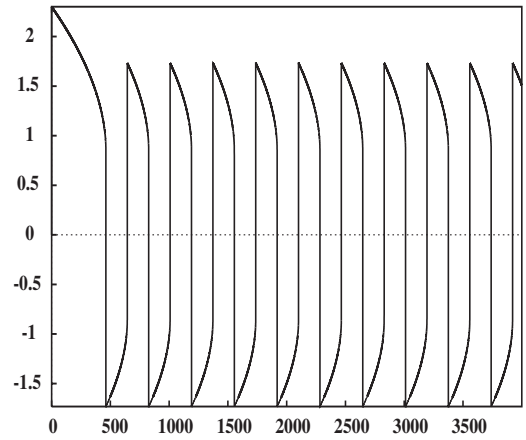

FIG. 5. *The time series plot for $v(t)$ of a relaxation oscillator* (2.2). *The natural frequency of oscillations is $\omega = 1$. The values of other parameters are the same as in Figure* 3.

$\overrightarrow{DA}$. The points B and D are referred as "jump points." This corresponds to the solution plotted in Figure 5. It can be shown that for $\epsilon > 0$ and sufficiently small the phase portrait of (2.1) has a smooth closed trajectory Z_ϵ that is $O(\epsilon)$ close to Z_0 in C^0-topology [14].

Another piece of information about a single relaxation oscillator that we need is its period. To leading order, the period T of the relaxation oscillations (2.2) is the same as that of the discontinuous solution Z_0 corresponding to the case of $\epsilon = 0$. The latter is equal to the sum of the traversal times for (2.2) on the slow motion segments $\overrightarrow{AB}$ and $\overrightarrow{CD}$ of Z_0. Suppose that at time $t = t_1$ the phase point of (2.2) is at point A of Z_0 (Figure 4) and $t = t_2$ is the time when it reaches the jump point B. The traversal time for the part AB is

$$T_{AB} = \int_{t_1}^{t_2} dt.$$

By differentiating both sides of the first equation in (2.5) with respect to the time variable and using the second one, we have

$$dt = \frac{1}{\omega} \frac{f'(v)}{v} dv$$

on the slow segments of Z_0. Therefore,

$$T_\omega^0 = T_{AB} + T_{CD} = \frac{1}{\omega} \int_{\tilde{Z}_0} \frac{f'(v)}{v} dv, \tag{2.6}$$

where $\tilde{Z}_0 \equiv (b_l, a_l) \bigcup (b_r, a_r)$ (Figure 4). The frequency of the oscillations of (2.2) to leading order is

$$\Lambda_\omega^0 = \omega \Lambda^0, \quad \text{where} \quad \Lambda^0 = \left(\int_{\tilde{Z}_0} \frac{f'(v)}{v} dv \right)^{-1}. \tag{2.7}$$

In what follows we will refer to ω as a natural frequency of the relaxation oscillator (2.2). For rigorous justification of the asymptotic calculation of the period of oscillations we refer to [14].

The term "synchronization" may have different meanings in the context of different systems. We want to clarify the meaning of synchronization applicable to the system (2.1). We give the definition of synchronization for a more general system (1.2). Our definition is similar to the definition of the *asymptotic synchronization* in [9].

DEFINITION 2.1. *A solution* $(v_1, u_1, v_2, u_2, \dots, v_N, u_N) \in \mathbb{R}^{2N}$ *of* (1.2) *is called* synchronous *if after some initial lag period* ν*, depending on the initial conditions, it satisfies*

$$|v_i(t) - v_j(t)| \le \sigma(d), \quad \lim_{d\to\infty} \sigma(d) = 0, \quad t > \nu, \quad 1 \le i, j \le N.$$

3. Heuristics: Geometry and asymptotics. We start to analyze (2.1) by decomposing into the fast and slow subsystems. The key question for (2.1) is how the compartments can synchronize, even though the natural frequencies are very different. Once one makes the numerically plausible ansatz that $|v_2 - v_1| = O\left(\frac{1}{d}\right)$, the essential clue to how this can happen comes from the geometry of the fast and slow subsystems of the coupled system (2.1). The decomposition is done in exactly the same way as for a single oscillator (2.2). Using the notation of the previous section, the reduced fast and slow subsystems are given by

$$\begin{aligned} \frac{dv_i}{d\tau} &= f(v_i) - u_i + d(v_j - v_i), \\ \frac{du_i}{d\tau} &= 0 \end{aligned} \tag{3.1}$$

and

$$\begin{aligned} u_i &= f(v_i) + d(v_j - v_i), \\ \frac{du_i}{dt} &= \omega_i v_i, \end{aligned} \tag{3.2}$$

respectively.

As in the case of a single relaxation oscillator, the singular solutions to a coupled system (2.1) are constructed as the unions of solutions of simpler fast and slow equations (3.1) and (3.2). For a two-dimensional relaxation oscillator (2.2), it is easy to construct the singular solution from the cubic-shaped nullclines of the fast variable u (Figure 4). The singular solution moves along this nullcline and jumps at each of its "knees," or local extrema of nullclines. For (2.1), the singular solution again moves along some submanifold, which is the slow manifold of (2.1) and jumps at the "jump" points. However, these slow manifolds and their boundaries are no longer as evident from the equations.

The ansatz

$$|v_2 - v_1| = O(\delta), \quad \delta \equiv \frac{1}{d}, \tag{3.3}$$

implies that the coupling terms $\pm d(v_2 - v_1)$ are $O(1)$. The slow manifold (first equation of (3.2)) is parametrized by v_1 and v_2, but along any given trajectory on the slow manifold v_1 and v_2 are related, so we can think of

$$d(v_2 - v_1) \equiv c(v_1), \tag{3.4}$$

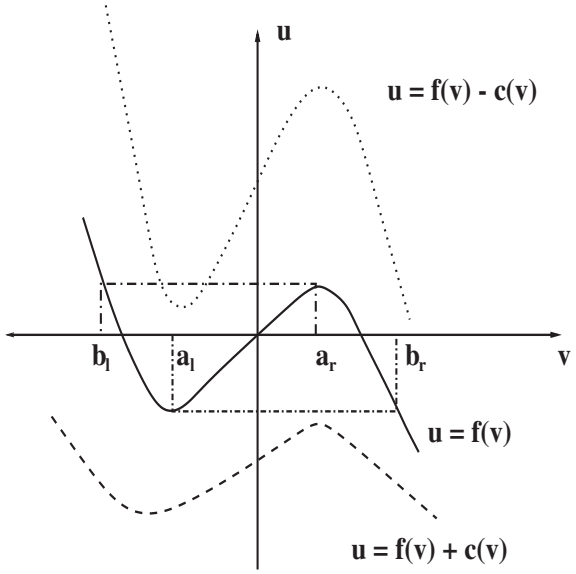

FIG. 6. *Two generalized nullclines Γ_1 (the dashed curve) and Γ_2 (the dotted curve) for the system of coupled oscillators* (2.1). *Note that the slow segments of Γ_1, the generalized nullcline of the slow oscillator ($\omega_1 < \omega_2$), are shorter than those of Γ_2, the generalized nullcline of the fast oscillator. This is consistent with the fact that two oscillators are synchronous.*

where $c(v_1)$ is an $O(1)$ function that depends on the particular trajectory. Then v_2 is given by

$$v_2 = v_1 + \delta d(v_2 - v_1) = v_1 + \delta c(v_1). \tag{3.5}$$

Along the slow trajectory, the variables then satisfy

$$\begin{aligned} u_1 &= f(v) + c(v), \\ u_2 &= f(v + \delta c(v)) - c(v), \end{aligned} \tag{3.6}$$

$$\begin{aligned} \frac{du_1}{dt} &= \omega_1 v, \\ \frac{du_2}{dt} &= \omega_2 (v + \delta c(v)). \end{aligned} \tag{3.7}$$

Here we have dropped the index of v_1 to simplify the notation.

To lowest order in δ, the geometry associated with (3.6) is shown schematically in Figure 6 for the right branch of the slow manifold. The solid curve represents the graph of $u = f(v)$, the dashed curve is given by $u = f(v) + c(v)$ and the dotted curve is given by $u = f(v) - c(v)$. $v = a_r$ is the value of v at which a knee is reached. (We show below that, to lowest order, the voltage value of this jump point is independent of the trajectory and the same for each compartment.) Note that in Figure 6, the interval in u corresponding to the trajectory between $v = b_r$ and $v = a_r$ is shorter for the dotted curve than for the dashed one. Such a geometry, for the correct function $c(v)$, is potentially consistent with (3.7), in the case $\omega_2 > \omega_1$. That is, if $c(v)$ changes with v in precisely the correct manner, it is possible to maintain v_1 approximately equal to v_2, even though $\omega_2 - \omega_1$ is $O(1)$.

In the asymptotics given below in this section, we show how to calculate such a trajectory-dependent function $c(v)$ for given initial conditions along the slow manifold. This will be used in later sections to construct a 1-parameter family of periodic solutions in the limits $\epsilon \to 0$ and $\delta \to 0$.

By differentiating both sides of (3.6) with respect to v, we find that

$$\begin{aligned} \frac{du_1}{dv} &= f'(v) + c'(v), \\ \frac{du_2}{dv} &= f'\left(v + \delta c(v)\right)\left(1 + \delta c'(v)\right) - c'(v). \end{aligned} \tag{3.8}$$

On the other hand, (3.7) yields

$$\begin{aligned} \frac{du_1}{dv} &= \omega_1 v \left(\frac{dv}{dt}\right)^{-1}, \\ \frac{du_2}{dv} &= \omega_2 \left(v + \delta c(v)\right) \left(\frac{dv}{dt}\right)^{-1}. \end{aligned} \tag{3.9}$$

Hence, by computing the ratio from (3.8) and (3.9) we obtain an ODE for $c(v)$:

$$\frac{f'(v) + c'(v)}{f'\left(v + \delta c(v)\right)\left(1 + \delta c'(v)\right) - c'(v)} = \frac{\omega_1 v}{\omega_2 \left(v + \delta c(v)\right)}. \tag{3.10}$$

It suffices for our purposes to calculate $c(v)$ up to $O(\delta)$. Thus, $f'\left(v + \delta c(v)\right)$ in (3.10) can be approximated by $f'(v) + \delta f''(v)c(v)$. By rearranging terms, (3.10) can be rewritten, up through terms of $O(\delta)$, as

$$\left(\omega_1 + \omega_2\right) v c' = \left(\omega_1 - \omega_2\right) v f' + \delta \left(\omega_1 f' c' v + \omega_1 f'' c v - \omega_2 f' c - \omega_2 c' c\right). \tag{3.11}$$

We use the ansatz (3.3) that we have adopted for the asymptotic analysis and (3.4) to expand $c(v)$ into the series

$$c(v) = \sum_{k=0}^{\infty} c_k(v) \delta^k, \tag{3.12}$$

where none of c_k's depends on δ. Plugging (3.12) in (3.11) and extracting only the $O(1)$ terms, we obtain the leading order equation:

$$O(1): \qquad c_0'(v) = \frac{\omega_1 - \omega_2}{\omega_1 + \omega_2} f'(v). \tag{3.13}$$

Thus,

$$c_0(v) = \frac{\omega_1 - \omega_2}{\omega_1 + \omega_2} f(v) + K, \tag{3.14}$$

where K is an arbitrary constant. The K encodes the dependence on initial conditions, which is given explicitly in the next section.

Similarly, by plugging (3.12) into (3.11) and selecting the terms of order $O(\delta)$ we have

$$O(\delta): \qquad \left(\omega_1 + \omega_2\right) v c_1' = \omega_1 f' c_0' v + \omega_1 f'' c_0 v - \omega_2 f' c_0 - \omega_2 c_0' c_0. \tag{3.15}$$

Equations (3.14) and (3.15) yield

$$c_1'(v) = \left(\frac{-2\omega_1\omega_2}{(\omega_1+\omega_2)^2}\frac{f'}{v} + \frac{\omega_1}{\omega_1+\omega_2} f'' \right) K - \frac{2\omega_1\omega_2(\omega_1-\omega_2)}{(\omega_1+\omega_2)^3}\frac{f'f}{v} + \frac{\omega_1(\omega_1-\omega_2)}{(\omega_1+\omega_2)^2}(f'f)'. \tag{3.16}$$

The asymptotic equations (3.14) and (3.16) will be used in the phase-space analysis of (2.1) to construct the periodic solution for finite coupling strength d.

4. Constructing a synchronous solution. Using the asymptotic calculation of the previous section, we can formally construct a synchronous solution to (2.1). We start out by approximating the dynamics on the slow manifolds.

4.1. The zeroth order approximation. By (3.6) and (3.14), the slow system to the lowest order of accuracy can be written as

$$\begin{aligned} u_1 &= \frac{2\omega_1}{\omega_1+\omega_2} f(v) + K, \\ u_2 &= \frac{2\omega_2}{\omega_1+\omega_2} f(v) - K, \\ \frac{du_1}{dt} &= \omega_1 v, \\ \frac{du_2}{dt} &= \omega_2 v, \end{aligned} \tag{4.1}$$

where by (3.14) K is an arbitrary constant.

The dynamics of the degenerate system (4.1) can be given a natural phase plane description. Denote

$$\Gamma_i(K) = \left\{ (v, u_i) : \quad u_i - \frac{2\omega_i}{\omega_1+\omega_2} f(v) + (-1)^i K = 0 \right\}, \quad i = 1, 2. \tag{4.2}$$

Two generalized nullclines Γ_1 and Γ_2 are as in Figure 6. Following standard terminology [14], we refer to those parts of Γ_i where $f'(v) < 0$ as *stable*. The constant K can be determined from the initial values $u_1(t_0)$ and $u_2(t_0)$. Using the top two equations in (4.1) we have

$$K = \frac{\omega_2 u_1(t_0) - \omega_1 u_2(t_0)}{\omega_1+\omega_2}. \tag{4.3}$$

We note that the geometry of the generalized nullclines (4.1) implies that both graphs of u_1 and u_2 as functions of v have the same points of maximum and minimum at $v = a_{r,l}$, which also are the extrema of $u = f(v)$ (Figure 6). Therefore, the jump points to leading order are the same for both oscillators and are independent of K. Moreover, it is straightforward to show that the same conclusion holds for the landing points $v = b_{r,l}$ (Figure 6). The latter are defined as the abscissas of the points of intersection of the horizontal lines of fast motion with the stable branches of the generalized nullclines $\Gamma_i(K)$ opposite to the branches from where the jumps occurred.

Now we are in a position to describe the singular dynamics of (2.1) as $\epsilon \to 0$ and $d \to \infty$. According to (4.1), phase points (v, u_1) and (v, u_2) will move upward (downward) along the right (left) stable branches of $\Gamma_1(K)$ and $\Gamma_2(K)$. Upon reaching

the jump point a_r (a_l) (Figure 6), there is a rapid change in the v coordinate along the lines with constant values of u_1 and u_2 in the direction of the opposite branch of the graph of $\Gamma_i(K)$. The dynamics on the opposite branches are then followed by the fast jumps. As a result, we obtain two closed trajectories $\gamma_i(K), i = 1, 2$, in (v_i, u_i) phase planes, corresponding to the zeroth order approximation of the synchronous oscillations of the coupled system (2.1). In fact, in the (v_1, u_1, v_2, u_2) phase space, we have a family of periodic solutions $(\gamma_1 \times \gamma_2)(K)$ parameterized by K.

4.2. The frequency of synchronous oscillations. We now compute the period of the synchronous oscillations of (2.1). In a manner similar to that shown in the case of a single oscillator (2.2), we have from (4.1)

$$dt = \frac{2}{\omega_1 + \omega_2} \frac{f'(v)}{v} dv \tag{4.4}$$

on the slow parts of $\gamma_i(K)$. Following exactly the same steps as in the analogous calculation of section 2, we obtain the period of synchronous oscillations

$$T^0_{(\omega_1,\omega_2)} = \frac{2}{\omega_1 + \omega_2} \int_{\tilde{Z}_0} \frac{f'(v)}{v} dv, \tag{4.5}$$

computed to leading order. Thus, the frequency of synchronous oscillations is

$$\Lambda^0_{(\omega_1,\omega_2)} = \frac{\omega_1 + \omega_2}{2} \Lambda^0, \tag{4.6}$$

where Λ^0 was defined in (2.7). The frequency is the same as that of the uncoupled oscillator (2.2) with natural frequency $\omega = \frac{\omega_1+\omega_2}{2}$. By (4.6) and (2.7), we conclude that the frequency of oscillations generated by the coupled system is the mean of the frequencies of the individual oscillators. In analogy to the case of a single relaxation oscillator, we refer to $\frac{\omega_1+\omega_2}{2}$ as the natural frequency of the coupled system to leading order.

Summing up the results of the zeroth order analysis, we conclude that it shows how to construct synchronous solutions of (2.1) to the lowest order. It also explains how the frequency of synchronous oscillations in the coupled system is generated by the natural frequencies of the individual oscillators and is independent of K. Moreover, from the zeroth order analysis, we can see why the time series plotted for u_1 and u_2 display different amplitudes of oscillations (Figure 3(b)). Indeed, by (4.1) the generalized nullclines Γ_1 and Γ_2 can be obtained from the v-nullcline Γ of a single relaxation oscillator (2.2) by multiplying it by the scaling factors $\frac{2\omega_{1,2}}{\omega_1+\omega_2}$, respectively. However, the zeroth order analysis does not explain the transient dynamics during which the system spirals up toward a unique limit cycle in the phase plane (Figure 3(a)). It also does not specify the value of K that corresponds to this unique stable limit cycle. Therefore, we need to perform the asymptotic analysis to the next order.

4.3. The first order analysis. According to the zeroth order asymptotic analysis, the phase points (v_1, u_1) and (v_2, u_2) follow closed orbits in the corresponding phase planes. However, the $O(\delta)$ terms in the governing equation (3.11) alter this picture. Indeed, suppose the phase points (v_1, u_1) and (v_2, u_2) at the start of the nth cycle (the moment when they hit the right-hand branch of the slow manifold) are located on the right branches of $\Gamma_{1,2}(K_n)$, respectively, for some K_n. Because of the $O(\delta)$ terms in the governing equation, as the phase points move along, they deviate from the nullclines $\Gamma_{1,2}(K_n)$. By the time they reach the jump points, they

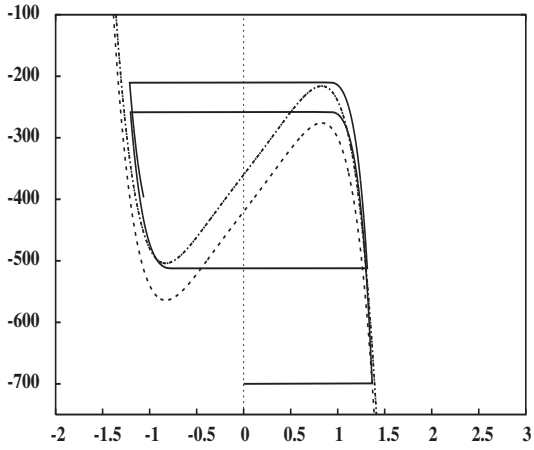

FIG. 7. *This figure shows a deviation of the phase point from the $O(1)$ periodic solution after going around one cycle. The generalized nullclines corresponding to the first and the second cycles (the dashed and dash-dotted curves, respectively) differ by a vertical shift. The asymptotic analysis yields that the magnitude of this shift is $O(\delta)$. The values of parameters for this figure were chosen so that the deviation of the phase point from the generalized nullcline is clearly seen. In particular, for this purpose the value of d was taken not very large.*

lie on $\Gamma_{1,2}(\hat{K}_n)$, for some $\hat{K}_n$, rather than on $\Gamma_{1,2}(K_n)$ (Figure 7). The constant $\hat{K}_n$ is $O(\delta)$ different from K_n. Similarly, after the phase points jump, they move along the left-hand stable branches of $\Gamma_{1,2}(\hat{K}_n)$, with some $O(\delta)$ deviation (see Figure 7). Therefore, after one full cycle, the phase points end up on the nullclines $\Gamma_{1,2}(K_{n+1})$, with constant K_{n+1}, which is $O(\delta)$ different from K_n.

We want to calculate the "drift" in K after one cycle:

$$\Delta_n K \equiv K_{n+1} - K_n. \tag{4.7}$$

Suppose that at the start of the nth cycle, the phase point (v_1, u_1) is on the right-hand stable branch of $\Gamma_1(K_n)$ for some K_n:

$$\begin{aligned} v_1 &= b_r, \\ u_1 &= \frac{2\omega_1}{\omega_1+\omega_2} f(b_r) + K_n. \end{aligned} \tag{4.8}$$

Using (3.8) and (3.12), we calculate u_1 at the time when v_1 or v_2 (whichever is first) has reached the jump point a_r:

$$\begin{aligned} u_1 &= \frac{2\omega_1}{\omega_1+\omega_2} f(b_r) + K_n + \int_{b_r}^{a_r^1} u_1' dv \\ &= \frac{2\omega_1}{\omega_1+\omega_2} f(b_r) + K_n + \int_{b_r}^{a_r^1} \left(f' + c_0'(v;K_n) + \delta c_1'(v;K_n)\right) dv + O(\delta^2). \end{aligned}$$

We let a_r^1 and a_l^1 denote the coordinates of the jump points computed to $O(\delta)$. Note that we have expanded the notation of $c(v)$ to $c(v;K)$ to make explicit the dependence of the function $c(v)$ on the parameter K; by $c'(v;K)$ we still denote the derivative with respect to v.

By (3.14), the last equation yields

$$u_1 = \frac{2\omega_1}{\omega_1+\omega_2} f(a_r^1) + K_n + \delta \int_{b_r}^{a_r^1} c_1'(v;K_n)dv + O(\delta^2) \equiv \frac{2\omega_1}{\omega_1+\omega_2} f(a_r^1) + \hat{K}_n. \tag{4.9}$$

The jump points are independent of K to $O(1)$ but not to $O(\delta)$. Note that on the picture we formed by neglecting the $O(\delta)$ terms, the projections of the phase point onto the $v_1 - u_1$ and $v_2 - u_2$ phase planes reach the jump points $a_{r,l}$ simultaneously (Figure 6), because $v_2 = v_1 \equiv v$ to leading order. However, if we add the $O(\delta)$ terms to the expressions for v_1 and v_2, they become

$$\begin{aligned} v_1 &= v, \\ v_2 &= v + \delta c(v). \end{aligned} \tag{4.10}$$

If $c(a_r)$ is negative, then v_2 will reach a_r before v_1, and therefore, the jump point on the right branch can be determined from the equation

$$v_2 = v + \delta c(v;K) = a_r, \quad \text{i.e.,} \quad a_r^1 + \delta c(a_r^1;K) = a_r.$$

This implies that, up to an error of $O(\delta^2)$, we have

$$a_r^1(K) = a_r - \delta c(a_r;K) = a_r - \delta\left(\frac{\omega_1-\omega_2}{\omega_1+\omega_2} f(a_r) + K\right). \tag{4.11}$$

If $c(a_r)$ is positive, then v_1 reaches a_r first and, as before, the two oscillators jump at $v = a_r^0$. Therefore,

$$a_r^1(K) = \min\left\{a_r, a_r - \delta c(a_r;K)\right\}.$$

Similarly,

$$a_l^1(K) = \max\left\{a_l, a_l - \delta c(a_l;K)\right\}.$$

We now continue to estimate $\Delta_n K$. Without introducing any $O(\delta)$ error we can change the upper limit of integration in the equation above to a_r, because $a_r - a_r^1 = O(\delta)$ according to (4.11). Therefore,

$$\hat{K}_n = K_n + \delta \int_{b_r}^{a_r} c_1'(v;K_n)dv + O(\delta^2). \tag{4.12}$$

Right after the jump, on the left stable branch of $\Gamma_1(\hat{K}_n)$ we have

$$\begin{aligned} v_1 &= b_l^1, \\ u_1 &= \frac{2\omega_1}{\omega_1+\omega_2} f(b_l^1) + \hat{K}_n. \end{aligned} \tag{4.13}$$

The value of u_1 does not change during the fast jump in the singular limit as $\epsilon \to 0$. Therefore, from (4.12) and (4.13) we conclude that $b_l^1 - b_l = O(\delta)$. In complete analogy to (4.9), on the left-hand branch of $\Gamma_1(K_n')$ we have

$$u_1 = \frac{2\omega_1}{\omega_1+\omega_2} f(a_l^1) + \hat{K}_n + \delta \int_{b_l^1}^{a_l^1} c_1'(v;\hat{K}_n)dv + O(\delta^2) \equiv \frac{2\omega_1}{\omega_1+\omega_2} f(a_l^1) + K_{n+1},$$

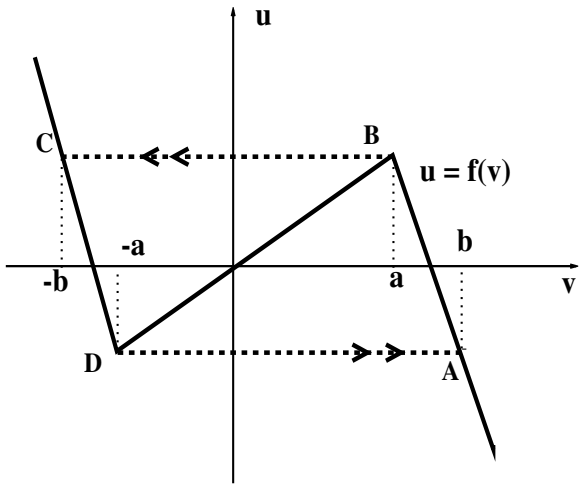

FIG. 8. *The phase plane for a relaxation oscillator with piecewise linear function $f(v)$.*

and therefore,

$$K_{n+1} = \hat{K}_n + \delta \int_{b_l}^{a_l} c_1'(v; \hat{K}_n) dv + O(\delta^2). \tag{4.14}$$

Here as before we have changed the limits of integration to b_l and a_l, because this does not contribute any $O(\delta)$ error.

By combining (4.12) and (4.14), we obtain that after one full cycle in the phase plane the drift in K is given by

$$K_{n+1} = K_n + \delta \int_{\tilde{Z}_0} c_1'(v; \hat{K}_n) dv + O(\delta^2), \quad \tilde{Z}_0 = (b_r^0, a_r^0) \bigcup (b_l^0, a_l^0). \tag{4.15}$$

From (4.15), one can see that the drift in K is $\Delta_n K \equiv K_{n+1} - K_n = O(\delta)$. Denote the principal term of the drift by

$$p(K_n) = \lim_{\delta \to 0} \frac{K_{n+1} - K_n}{\delta}. \tag{4.16}$$

Then to the lowest order we have a map

$$K_{n+1} = K_n + \delta p(K_n), \quad p(K_n) = \int_{\tilde{Z}_0} c_1'(v; \hat{K}_n) dv. \tag{4.17}$$

Attracting fixed points of the map (4.17) yield the values of K for (4.1) corresponding to the stable limit cycles of (2.1) to the lowest order. Thus, we have reduced the problem of constructing stable synchronous solutions of (2.1) to that of showing the fixed points of (4.17) are stable. Moreover, we note that if such attracting fixed points exist, then the iterations will converge to them with the rate proportional to $\delta \equiv \frac{1}{d}$. Thus, it will take longer to converge for large d.

4.4. An explicit example. We now illustrate the analysis of this section with an explicit example. In particular, we take f of the following form (Figure 8):

$$f(x) = \begin{cases} -\alpha x - \beta, & x \le -a, \\ \left(-\alpha + \frac{\beta}{a}\right) x, & -a < x < a, \\ -\alpha x + \beta & \text{otherwise}, \end{cases} \tag{4.18}$$

where $\alpha, \beta > 0$ and $0 < a < \frac{\beta}{\alpha}$. All calculations can be carried out, possibly with a greater effort, for other piecewise smooth functions f.

With this choice of $f(v)$, the equation (3.16) c_1' takes the following form:

$$c_1'(v;K) = \frac{-2\alpha\omega_1\omega_2}{(\omega_1+\omega_2)^2}\frac{K}{v} \pm \frac{2\alpha\beta\omega_1\omega_2(\omega_1-\omega_2)}{(\omega_1+\omega_2)^3} + \frac{\alpha^2\omega_1(\omega_1-\omega_2)}{(\omega_1+\omega_2)^3}. \tag{4.19}$$

Here, the $\pm$ sign in front of the second term on the right is chosen for the right/left stable branch of $\Gamma_1(K)$. By (4.16) and (4.19), we have

$$p(K_n) = \int_{(b,a)\cup(-b,-a)} c_1'(v;K_n)dv = \frac{-4\alpha\omega_1\omega_2}{(\omega_1+\omega_2)^2}(\ln b - \ln a)K_n, \tag{4.20}$$

where a is defined in (4.18) and $b = f^{-1}(-a)/\{-a\}$. Note that the particularly simple form of (4.20) is a consequence of the odd symmetry of the function $f(v)$. Hence, up to $O(\delta^2)$ terms, we obtain the following map:

$$K_{n+1} = (1+\delta L)K_n, \quad L = \frac{-4\alpha\omega_1\omega_2}{(\omega_1+\omega_2)^2}(\ln b - \ln a). \tag{4.21}$$

The map (4.21) is a linear map. It has a unique fixed point at the origin. Moreover, this is an attracting fixed point because $L < 0$. The rate at which iterations converge to the fixed point is, therefore, δL, i.e., $\frac{L}{d}$. Hence, the convergence is slow for strong coupling.

5. Constructing a Lyapunov function for a chain of two oscillators. As we have seen in the previous section, a direct asymptotic calculation, though useful for a system of two oscillators, is cumbersome and therefore would be difficult to apply chains with more oscillators and more general kinetics. This motivates us to develop another method of analysis that would be applicable to a wide class of problems. The phase plane description that follows from the zeroth order asymptotic analysis reveals a family of periodic solutions. The phase portrait is similar to that of a conservative system. The $O(\delta)$ corrections can be considered as perturbations. The perturbed system no longer resembles a conservative one, and instead of a family of periodic solutions it has a unique stable limit cycle. In the light of this interpretation, it is natural to look for "energy" functional of the unperturbed "conservative-like" system and to check whether it can be used as a Lyapunov function for the perturbed system. This is the strategy of the analysis presented in this section. In section 6 we will show that the same approach works well for the chains of N oscillators.

We continue to study (2.1). Suppose that the phase point (v_1, u_1, v_2, u_2) is in an $O(\delta)$ vicinity of the limit cycle $(\gamma_1 \times \gamma_2)(K)$, corresponding to some real K. As before, we assume (3.3), i.e., v_1 and v_2 are $O(\delta)$ distance apart. We introduce a function

$$L(u_1,u_2) \equiv \frac{1}{2}\left(\frac{u_1}{\omega_1} - \frac{u_2}{\omega_2} + A\right)^2, \tag{5.1}$$

where

$$A = \frac{1}{T}\frac{\omega_1-\omega_2}{\omega_1\omega_2}\oint f(v(t))dt,$$

T is a period of oscillations, and $\oint$ denotes the integral over one cycle. Using (4.4), the expression for A can also be rewritten as

$$A = \frac{1}{T}\frac{\omega_1-\omega_2}{\omega_1\omega_2}\frac{2}{\omega_1+\omega_2}\int_{\tilde{Z}_0}\frac{ff'}{v}dv.$$

Using (4.1), we evaluate L along the singular orbit $(\gamma_1 \times \gamma_2)(K)$:

$$L(u_1, u_2) \equiv L(K) = \frac{1}{2}\left(\frac{\omega_1+\omega_2}{\omega_1\omega_2}K + A\right)^2.$$

Clearly, $L(\bar{K}) = 0$, where

$$\bar{K} = \frac{-1}{T}\frac{\omega_1-\omega_2}{\omega_1+\omega_2}\oint f(v(t))\,dt = -\frac{1}{T}\frac{2(\omega_1-\omega_2)}{(\omega_1+\omega_2)^2}\int_{\tilde{Z}}\frac{ff'}{v}dv, \tag{5.2}$$

and $L(K) > 0$ is strictly positive otherwise.

Differentiation of L with respect to the time variable t yields

$$\frac{dL}{dt} = \left(\frac{u_1}{\omega_1} - \frac{u_2}{\omega_2} + A\right)\left(\omega_1^{-1}\frac{du_1}{dt} - \omega_2^{-1}\frac{du_2}{dt}\right). \tag{5.3}$$

By (4.1), on the slow segments we have

$$\frac{dL}{dt} = \left(\frac{\omega_1+\omega_2}{\omega_1\omega_2}K + A\right)(v_1 - v_2). \tag{5.4}$$

Furthermore, the combination of (3.4) and (3.14) yields

$$v_1 - v_2 = -\delta c(v_1) = -\delta\left(\frac{\omega_1-\omega_2}{\omega_1+\omega_2}f(v_1) + K\right). \tag{5.5}$$

By plugging (5.5) into (5.4) and after carrying out some algebra we find that

$$\frac{dL}{dt} = -\delta\frac{\omega_1\omega_2}{\omega_1+\omega_2}\left(\frac{\omega_1+\omega_2}{\omega_1\omega_2}K + A\right)\left(\frac{\omega_1+\omega_2}{\omega_1\omega_2}K + \frac{\omega_1-\omega_2}{\omega_1\omega_2}f(v)\right). \tag{5.6}$$

From (5.6), we compute to leading order the change in L after one cycle:

$$\Delta L(K) = \oint\frac{dL}{dt}dt = -\delta\frac{\omega_1\omega_2}{\omega_1+\omega_2}T\left(\frac{\omega_1+\omega_2}{\omega_1\omega_2}K + A\right)^2 \le 0. \tag{5.7}$$

Therefore, L can be viewed as an analog of the Lyapunov function for (2.1). Moreover, we can estimate the rate of convergence of the solution to the steady-state oscillations (corresponding to $L = 0$) by noting that

$$\frac{\Delta L}{T} = -\delta\lambda L, \quad \lambda = \frac{2\omega_1\omega_2}{\omega_1+\omega_2}. \tag{5.8}$$

If we average ΔL uniformly over the whole cycle, L can be interpolated by the solution of the initial value problem:

$$\begin{aligned}\frac{d\tilde{L}}{dt} &= -\delta\lambda\tilde{L},\\ \tilde{L}(0) &= L(0).\end{aligned} \tag{5.9}$$

Therefore,

$$\tilde{L}(t) = L(0)e^{-\delta\lambda t}. \tag{5.10}$$

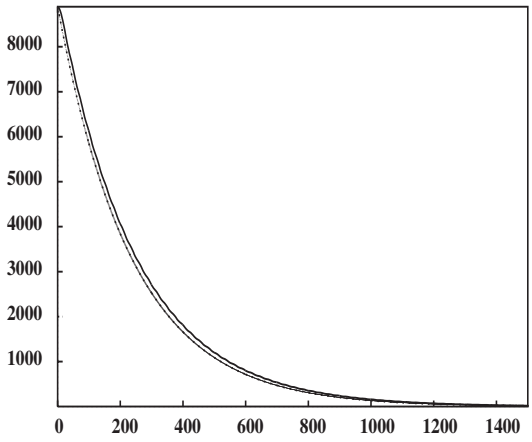

FIG. 9. *Numerically computed (upper curve) and theoretically predicted (lower curve) plots of the Lyapunov function, $L(t)$, for a system of two coupled oscillators* (2.1).

Equations (5.8) and (5.10) show that the system approaches the steady-state oscillations with rate dependent on δ. These equations explain numerical observations that the transition period is longer for strong coupling $d = \frac{1}{\delta}$.

We illustrate the results of this section with a numerical example. The upper curve plotted in Figure 9 corresponds to the values of L evaluated numerically along the trajectory of (2.1). The analytical prediction $\tilde{L}$ by (5.10) is given by the lower curve. One can see a good fit between theses two curves. The error is mainly due to the error of estimating the initial value $L(0)$.

Therefore, in this section we have recovered the results of section 4. The advantage of the use of Lyapunov function is that it frees us from the cumbersome analysis to the first order. This approach can also be applied to analyze the chains with more oscillators. This will be done in the next section.

6. Analyzing a chain of *N* oscillators. The numerical simulations for chains of many relaxation oscillators of type (2.1) show the dynamical patterns similar to those that we have studied for two coupled oscillators (Figure 10). In the present section, we will apply the approach worked out for chains of two coupled oscillators to chains of N oscillators (1.2).

6.1. The zeroth order analysis. In a singular limit as $\epsilon \to 0$, we separate the dynamics of (1.2) into the fast and slow motions and assume that

$$v_{i+1} - v_i = O(\delta), \quad i = 1, 2, \dots, N-1. \tag{6.1}$$

The natural generalizations of functions $c_i(v)$ are

$$c_i(v_1) \equiv d(v_{i+1} - v_i), \quad i = 1, 2, \dots, N-1, \tag{6.2}$$

where $(\boldsymbol{v}, \boldsymbol{u}) = (v_1, v_2, \dots, v_N, u_1, u_2, \dots, u_N)$ belongs to the phase trajectory of (1.2). As before, the functions $c_i(v_1)$ need to be redefined for each period. For given initial conditions $(\boldsymbol{v}^0, \boldsymbol{u}^0)$ we denote the trajectory of (1.2) by $Z_{\epsilon,\delta} = (\boldsymbol{v}(t), \boldsymbol{u}(t))$.

We assume that the trajectory $Z_{\epsilon,\delta}$ does not leave the bounded domain $D \subset \mathbb{R}^{2N}$ with diameter $M > 0$. Throughout the paper, by $\|\cdot\|$ we shall denote the L^∞

norms of scalar and vector functions of one variable defined on the closed interval $I = [-M-1, M+1]$. For instance,

$$\|f\| \equiv \max_I |f(v_1)|, \|\boldsymbol{c}\| \equiv \max_{1\le k\le N-1} \max_I |c_k(v_1)|,$$
$$\text{where } \boldsymbol{c}(v_1) = (c_1(v_1), c_2(v_1), \dots, c_{N-1}(v_1))^T.$$

Note that (6.1) and (6.2) imply that $\|\boldsymbol{c}\|$ is uniformly bounded as $\delta \to 0$.

From the assumptions above, it follows that

$$v_i = v_1 + \sum_{k=1}^{i-1} (v_{k+1} - v_k) = v_1 + \delta \sum_{k=1}^{i-1} c_k(v_1),$$
$$f(v_i) = f\left(v_1 + \delta \sum_{k=1}^{i-1} c_k(v_1)\right), \quad i = 2, 3, \dots, N.$$

Therefore,

$$|v_i - v_1| \le \delta N \|\boldsymbol{c}\|, \tag{6.3}$$
$$|f(v_i) - f(v_1)| \le \delta N \|f'\| \|\boldsymbol{c}\|, \quad i = 2, 3, \dots, N.$$

The slow equations now can be rewritten as

$$\begin{aligned} u_1 &= f(v_1) + c_1(v_1), \\ u_i &= f(v_1) + c_i(v_1) - c_{i-1}(v_1) + \{f(v_i) - f(v_1)\} \\ &= f(v_1) + c_i(v_1) - c_{i-1}(v_1) + \delta\mu_i(v_1), \quad i = 2, 3, \dots, N-1, \\ u_N &= f(v_1) - c_{N-1}(v_1) + \{f(v_{N-1}) - f(v_1)\} = f(v_1) - c_{N-1}(v_1) + \delta\mu_N(v_1), \\ \frac{du_i}{dt} &= \omega_i v_1 + \omega_i v_i - v_1 = \omega_i v_1 + \delta\nu_i(v_1), \quad i = 1, 2, \dots, N. \end{aligned} \tag{6.4}$$

It is convenient to have (6.4) rewritten in a vector form:

$$\boldsymbol{u} = \boldsymbol{f}(v_1) + \boldsymbol{S}\boldsymbol{c}(v_1) + \delta\boldsymbol{\mu}(v_1), \tag{6.5}$$

$$\frac{d\boldsymbol{u}}{dt} = v_1\boldsymbol{\omega} + \delta\boldsymbol{\nu}(v_1), \tag{6.6}$$

where

$$\begin{aligned} \boldsymbol{f}(v_1) &= (f(v_1), f(v_1), \dots, f(v_1))^T, \quad \boldsymbol{\omega} = (\omega_1, \omega_2, \dots, \omega_N)^T, \\ \boldsymbol{\mu}(v_1) &= (\mu_1(v_1), \mu_2(v_1), \dots, \mu_N(v_N))^T, \quad \boldsymbol{\nu}(v_1) = (\nu_1(v_1), \nu_2(v_1), \dots, \nu_N(v_N))^T \in \mathbb{R}^N, \end{aligned}$$

and $\boldsymbol{S}$ is an $N \times (N-1)$ matrix

$$\boldsymbol{S} = \begin{pmatrix} 1 & 0 & 0 & 0 & \dots & \dots & 0 & 0 \\ -1 & 1 & 0 & 0 & \dots & \dots & 0 & 0 \\ 0 & -1 & 1 & 0 & \dots & \dots & 0 & 0 \\ \vdots & \vdots & \vdots & \vdots & \vdots & \dots & \vdots & \vdots \\ 0 & 0 & 0 & 0 & \dots & \dots & -1 & 1 \\ 0 & 0 & 0 & 0 & \dots & \dots & 0 & -1 \end{pmatrix}. \tag{6.7}$$

Estimates (6.3) and equations (6.5) imply that

$$\|\boldsymbol{\mu}\| \le \delta N \|\boldsymbol{f}'\| \|\boldsymbol{c}\| = O(\delta), \qquad \|\boldsymbol{\nu}\| \le \delta N \bar{\omega} \|\boldsymbol{c}\| = O(\delta). \tag{6.8}$$

By differentiating the equation for u_i in (6.4) with respect to v_1 we obtain

$$\frac{du_i}{dv_1} = f'(v_1) + c_i'(v_1) - c_{i-1}'(v_1) + \delta\mu_i{}'(v_1), \quad i = 2, 3, \dots, N-1. \tag{6.9}$$

On the other hand, using the last equation of (6.4) we have

$$\frac{du_i}{dv_1} = (\omega_i v_1 + \delta\nu_i{}'(v_1)) \left(\frac{dv_1}{dt}\right)^{-1}, \quad i = 1, 2, \dots, N. \tag{6.10}$$

We divide the equation for u_{i+1} by the equation for u_i in (6.9) and take a similar ratio in (6.10). By setting these two ratios equal we obtain

$$\frac{f'(v_1) + c_{i+1}'(v_1) - c_i'(v_1)}{f'(v_1) + c_i'(v_1) - c_{i-1}'(v_1)} = \frac{\omega_{i+1}}{\omega_i} + \delta\sigma_i(v_1), \tag{6.11}$$

where all the $O(\delta)$ terms are included in $\delta\sigma_i(v_1)$.

Similarly,

$$\frac{f'(v_1) + c_2'(v_1) - c_1'(v_1)}{f'(v_1) + c_1'(v_1)} = \frac{\omega_2}{\omega_1} + \delta\sigma_1(v_1) \tag{6.12}$$

$$\text{and} \quad \frac{f'(v_1) - c_{N-1}'(v_1)}{f'(v_1) + c_{N-1}'(v_1) - c_{N-2}'(v_1)} = \frac{\omega_N}{\omega_{N-1}} + \delta\sigma_{N-1}(v_1).$$

After some algebra, the combination of (6.11) and (6.12) yields

$$\mathbf{\Lambda} \boldsymbol{c}'(v_1) = f'(v_1)\boldsymbol{\theta} + \delta\boldsymbol{\sigma}(v_1), \quad \boldsymbol{\sigma} = (\sigma_1, \sigma_2, \dots, \sigma_{N-1}), \tag{6.13}$$

where an $(N-1) \times (N-1)$ matrix $\mathbf{\Lambda}$ is given by

$$\mathbf{\Lambda} = \begin{pmatrix} 1 & \frac{-\omega_1}{\omega_1+\omega_2} & 0 & 0 & \dots & \dots & \dots & \dots & \dots & \dots & 0 \\ \frac{-\omega_3}{\omega_2+\omega_3} & 1 & \frac{-\omega_2}{\omega_2+\omega_3} & 0 & \dots & \dots & \dots & \dots & \dots & \dots & 0 \\ \vdots & & & \vdots & & & \vdots & & \vdots & & \vdots \\ 0 & 0 & \dots & \dots & 0 & \frac{-\omega_{i+1}}{\omega_i+\omega_{i+1}} & 1 & \frac{-\omega_i}{\omega_i+\omega_{i+1}} & 0 & \dots & 0 \\ \vdots & & & \vdots & & & \vdots & & \vdots & & \vdots \\ 0 & 0 & \dots & \dots & \dots & \dots & \dots & \dots & \dots & \frac{-\omega_N}{\omega_{N-1}+\omega_N} & 1 \end{pmatrix},$$

$$\boldsymbol{\theta} = (\theta_1, \theta_2, \dots, \theta_{N-1})^T, \quad \theta_i = \frac{\omega_i - \omega_{i+1}}{\omega_i + \omega_{i+1}}, \quad i = 1, 2, \dots, N-1.$$

Note that under the assumptions made in the beginning of this section the term $\|\boldsymbol{\sigma}\|$ is uniformly bounded as $\delta \to 0$. By setting $\delta = 0$ we obtain an unperturbed problem:

$$\mathbf{\Lambda} \boldsymbol{c}_0'(v_1) = f'(v_1)\boldsymbol{\theta}. \tag{6.14}$$

PROPOSITION 6.1. *If $\omega_i > 0, i = 1, 2, \dots, N$, then the matrix $\mathbf{\Lambda}$ is nonsingular.*

Proof. By induction in N, one can prove that

$$\det\mathbf{\Lambda} = \frac{\omega_2\omega_3 \dots \omega_{N-1}(\omega_1 + \omega_2 + \dots + \omega_N)}{(\omega_1 + \omega_2)(\omega_2 + \omega_3) \dots (\omega_{N-1} + \omega_N)}. \qquad \square$$

Because $\mathbf{\Lambda}$ is nonsingular, there exists a unique solution $\boldsymbol{\xi} = (\xi_1, \xi_2, \ldots, \xi_{N-1})^T$ to the system of algebraic equations

$$\mathbf{\Lambda}\boldsymbol{\xi} = \boldsymbol{\theta}. \tag{6.15}$$

Consequently, $\boldsymbol{c}_0'(v_1) = f'(v_1)\boldsymbol{\xi}$. The latter yields

$$\boldsymbol{c}_0(v_1) = f(v_1)\boldsymbol{\xi} + \boldsymbol{K}, \quad \boldsymbol{K} = (K_1, K_2, \ldots, K_{N-1}). \tag{6.16}$$

By plugging (6.16) into (6.5) with $\delta = 0$ we obtain the zeroth order approximation of the slow equations:

$$\begin{aligned} \boldsymbol{u} &= (\boldsymbol{I} + \boldsymbol{S}\boldsymbol{\xi})\boldsymbol{f}(v_1) + \boldsymbol{S}\boldsymbol{K}, \\ \frac{d\boldsymbol{u}}{dt} &= v_1 \boldsymbol{I}\boldsymbol{\omega}, \end{aligned} \tag{6.17}$$

where $\boldsymbol{I}$ stands for the $N \times N$ identity matrix.

In analogy to the analysis of a chain of two oscillators given in section 4.1 we show that the relations (6.17) yield a family of synchronous solutions to (1.2) as $d \to \infty$. This has the following phase plane description. Since the argument almost literally repeats that of section 4, we only outline it.

Denote

$$\begin{aligned} \Gamma_1(K) &= \{(u_1, v_1): \quad u_1 - (1+\xi_1)f(v_1) - K_1 = 0\}, \\ \Gamma_i(K) &= \{(u_i, v_i): \quad u_i - (1+\xi_i - \xi_{i-1})f(v_i) - K_i + K_{i+1} = 0\},\ i = 2, 3, \ldots, N-1, \\ \Gamma_N(K) &= \{(u_N, v_N): \quad u_N - (1-\xi_N)f(v_N) + K_N = 0\}. \end{aligned}$$

We refer to the parts of Γ_i, where $f'(v) < 0$ as *stable*. As in the case of a single relaxation oscillator, the extrema a_l and a_r of $f(v)$ are called the left and right jump points, respectively.

According to (6.17), the phase points will follow upward (downward) the right (left) stable branches of $\Gamma_i(K)$. As before, we determine $\boldsymbol{K}$ from the initial data $\boldsymbol{u}(t_0)$. We divide the ith equation in (6.17) by ω_i, $i = 1, 2, \ldots, N$, and subtract the $(j+1)$st equation from the equation j, $j = 1, 2, \ldots, N-1$. After some algebra (for details see (6.27) and (6.28)), for $t = t_0$ this results in the linear system for $\boldsymbol{K}$:

$$\mathbf{\Lambda}\boldsymbol{K} = \boldsymbol{h}\left(\boldsymbol{u}(t_0)\right), \tag{6.18}$$

where $\boldsymbol{h} = (h_1, h_2, \ldots, h_{N-1})^T$, $h_i(u) = \frac{u_{i+1}}{\omega_{i+1}} - \frac{u_i}{\omega_i}$, $i = 1, 2, \ldots, N-1$, and $\mathbf{\Lambda}$ was defined in (6.13). The vector $\boldsymbol{K}$ is uniquely defined by (6.18) because $\mathbf{\Lambda}$ is nonsingular.

All v_i components remain equal to v_1 to leading order. When the phase points reach the jump point $v = a_r(a_l)$ in the $v_i - u_i$ phase planes they jump instantaneously to the opposite stable branches of Γ_i. By repeating the argument of section 4, we find that the phase points land on the opposite branches of Γ_i corresponding to the same value of $\boldsymbol{K}$ and the landing points have coordinates

$$b_{r,l} = f^{-1}(a_{l,r})/\{a_{l,r}\}.$$

Thus, in the limit as $d \to \infty$ we have an $(N-1)$-parameter family of periodic orbits

$$\boldsymbol{\gamma}(\boldsymbol{K}) = (\gamma_1 \times \gamma_2 \times \cdots \times \gamma_N)(\boldsymbol{K}). \tag{6.19}$$

DEFINITION 6.2. *By $Z_{0,0}(\boldsymbol{K})$ we shall denote the singular ($\epsilon = \delta = 0$) trajectory constructed as an alternating sequence of segments of slow motions* (6.17) *and instantaneous jumps as described above. The constant $\boldsymbol{K}$ is determined from the initial conditions following* (6.18).

6.2. The frequency of synchronous oscillations. We now determine the period of the synchronous oscillations. Note that the rows of $\boldsymbol{S}$ add up to the zero row. Therefore, summing up the N top equations in (6.17) results in

$$\frac{u_1+u_2+\cdots+u_N}{N}=f(v). \tag{6.20}$$

By differentiating (6.20) with respect to t and using the last N equations in (6.17) we have

$$dt=\left(\frac{N}{\omega_1+\omega_2+\cdots+\omega_N}\right)\frac{f'(v)}{v}dv, \tag{6.21}$$

where we have dropped the index of v_1 to simplify the notation. Thus, to leading order

$$\begin{aligned} T^0_{(\omega_1,\omega_2,\dots,\omega_N)}&=\int_{\tilde Z_0}dt=\left(\frac{\omega_1+\omega_2+\cdots+\omega_N}{N}\right)^{-1}\int_{\tilde Z_0}\frac{f'(v)}{v}dv,\\ \tilde Z_0&=(b_r,a_r)\bigcup(b_l,a_l), \end{aligned} \tag{6.22}$$

and the frequency is

$$\Lambda^0_{(\omega_1,\omega_2,\dots,\omega_N)}=\frac{\omega_1+\omega_2+\cdots+\omega_N}{N}\Lambda^0, \tag{6.23}$$

where Λ^0 is defined in (2.7). As we expected, the natural frequency of synchronous solutions of the coupled system is to the lowest order the mean of the natural frequencies of the individual subsystems.

6.3. Constructing a Lyapunov function. To account for the deviation from the zeroth order dynamics of (1.2) we construct a Lyapunov function for the system of N oscillators:

$$L(u_1,u_2,\dots,u_N)=\frac12\sum_{i=1}^{N-1}\left(\frac{u_i}{\omega_i}-\frac{u_{i+1}}{\omega_{i+1}}+A_i\right)^2, \tag{6.24}$$

where

$$\begin{aligned} A_i&=\frac{\omega_i-\omega_{i+1}}{\omega_i\omega_{i+1}}B,\\ B&=\frac{1}{T}\oint f(v(t))dt=\frac{1}{T}\left(\frac{1}{N}\sum_{k=1}^{N}\omega_k\right)^{-1}\int_{\tilde Z^0}\frac{f'(v)f(v)}{v}dv. \end{aligned} \tag{6.25}$$

Next, we want to evaluate L on the singular orbits whose slow parts are given by (6.17). In preparation for this we derive a few auxiliary identities. We start with

$$\begin{aligned} \frac{u_i}{\omega_i}-\frac{u_{i+1}}{\omega_{i+1}}&=\left(\frac{1+\xi_i-\xi_{i-1}}{\omega_i}-\frac{1+\xi_{i+1}-\xi_i}{\omega_{i+1}}\right)f(v)\\ &\quad+\frac{K_i-K_{i-1}}{\omega_i}-\frac{K_{i+1}-K_i}{\omega_{i+1}},\quad i=2,3,\dots,N-2. \end{aligned} \tag{6.26}$$

By rearranging terms in (6.26) we obtain

$$\frac{u_i}{\omega_i} - \frac{u_{i+1}}{\omega_{i+1}} = \left[-\frac{\omega_{i+1}}{\omega_i\omega_{i+1}}\xi_{i-1} + \frac{\omega_i+\omega_{i+1}}{\omega_i\omega_{i+1}}\xi_i - \frac{\omega_i}{\omega_i\omega_{i+1}}\xi_{i+1} - \frac{\omega_i-\omega_{i+1}}{\omega_i\omega_{i+1}} \right] f + \left(-\frac{\omega_{i+1}}{\omega_i\omega_{i+1}}K_{i-1} + \frac{\omega_i+\omega_{i+1}}{\omega_i\omega_{i+1}}K_i - \frac{\omega_i}{\omega_i\omega_{i+1}}K_{i+1} \right).$$

The sum in the square brackets is equal to zero, because $\boldsymbol{\xi}$ solves (6.15). Thus, we have

$$\frac{u_i}{\omega_i} - \frac{u_{i+1}}{\omega_{i+1}} = -\frac{\omega_{i+1}}{\omega_i\omega_{i+1}}K_{i-1} + \frac{\omega_i+\omega_{i+1}}{\omega_i\omega_{i+1}}K_i - \frac{\omega_i}{\omega_i\omega_{i+1}}K_{i+1} \tag{6.27}$$

for $i = 2, 3, \ldots, N-2$. Similarly, one can show

$$\begin{aligned} \frac{u_1}{\omega_1} - \frac{u_2}{\omega_2} &= \frac{\omega_1+\omega_2}{\omega_1\omega_2}K_1 - \frac{\omega_1}{\omega_1\omega_2}K_2, \\ \frac{u_{N-1}}{\omega_{N-1}} - \frac{u_N}{\omega_N} &= \frac{\omega_{N-1}+\omega_N}{\omega_{N-1}\omega_N}K_{N-1} - \frac{\omega_N}{\omega_{N-1}\omega_N}K_{N-2}. \end{aligned} \tag{6.28}$$

By plugging (6.27) and (6.28) into (6.24), we find that along the singular orbits (6.17)

$$\begin{aligned} L(\boldsymbol{u}) \equiv L(\boldsymbol{K}) = {} & \frac{1}{2}\left(\frac{\omega_1+\omega_2}{\omega_1\omega_2}K_1 - \frac{\omega_1}{\omega_1\omega_2}K_2 + A_1 \right)^2 \\ & + \frac{1}{2}\sum_{i=1}^{N-2}\left(-\frac{\omega_{i+1}}{\omega_i\omega_{i+1}}K_{i-1} + \frac{\omega_i+\omega_{i+1}}{\omega_i\omega_{i+1}}K_i - \frac{\omega_i}{\omega_i\omega_{i+1}}K_{i+1} + A_i \right)^2 \\ & + \frac{1}{2}\left(\frac{\omega_N+\omega_{N-1}}{\omega_{N-1}\omega_N}K_{N-1} - \frac{\omega_N}{\omega_{N-1}\omega_N}K_{N-2} + A_{N-1} \right)^2, \end{aligned} \tag{6.29}$$

where A_i for $i = 1, 2, \ldots, N-1$ is defined in (6.25). The equation above implies that $L(\boldsymbol{K}) \geq 0$. Moreover, the combination of (6.29) and the definition of the matrix $\boldsymbol{\Lambda}$ (6.13) yields that

$$L(\bar{\boldsymbol{K}}) = 0, \quad \bar{\boldsymbol{K}} = -B\boldsymbol{\xi}. \tag{6.30}$$

Using (6.15), (6.29), and (6.30), we conclude that

$$L(\boldsymbol{K}) = 0 \quad \text{if} \quad \boldsymbol{K} = \bar{\boldsymbol{K}} \equiv -B\boldsymbol{\xi}$$

and $L(\boldsymbol{K}) > 0$ otherwise.

We want to show that the system evolves toward a limit cycle $\boldsymbol{\gamma}(\bar{\boldsymbol{K}}) \equiv (\gamma_1 \times \gamma_2 \times \cdots \times \gamma_N)(\bar{\boldsymbol{K}})$, on which L assumes its minimum value $L(\bar{\boldsymbol{K}}) = 0$. For this, we compute the change of L after a phase point has gone around $\boldsymbol{\gamma}(\boldsymbol{K})$:

$$\Delta L(\boldsymbol{K}) = \oint \frac{dL}{dt}dt.$$

Proposition 6.3.

$$\Delta L(\boldsymbol{K}) = -\delta G T(\boldsymbol{K}),$$

where

$$G(\boldsymbol{K}) \equiv P(\boldsymbol{y},\boldsymbol{y}) = \frac{y_1^2}{\omega_1} + \sum_{k=1}^{N-2} \frac{(y_k - y_{k+1})^2}{\omega_{k+1}} + \frac{y_{N-1}^2}{\omega_N} \geq 0 \tag{6.31}$$

and $\boldsymbol{y} = (y_1, y_2, \ldots, y_{N-1})^T$, $y_i = K_i + \xi_i B$.

Proof. Using (6.24), the last N equations in (6.4), and (6.2), we find that

$$\begin{aligned} \frac{dL}{dt} &= \sum_{i=1}^{N-1} \left(\frac{u_i}{\omega_i} - \frac{u_{i+1}}{\omega_{i+1}} + A_i \right) \left(\omega_i^{-1} \frac{du_i}{dt} - \omega_{i+1}^{-1} \frac{du_{i+1}}{dt} \right) \\ &= -\sum_{i=1}^{N-1} \left(\frac{u_i}{\omega_i} - \frac{u_{i+1}}{\omega_{i+1}} + A_i \right) (v_{i+1} - v_i) \\ &= -\delta \sum_{i=1}^{N-1} \left(\frac{u_i}{\omega_i} - \frac{u_{i+1}}{\omega_{i+1}} + A_i \right) c_i(v). \end{aligned} \tag{6.32}$$

Next, we plug (6.16) and (6.17) in (6.32) and integrate over one full cycle to obtain

$$\Delta L(\boldsymbol{K}) = \oint \frac{dL}{dt} dt = -\delta T G(\boldsymbol{K}), \tag{6.33}$$

where

$$\begin{aligned} G(\boldsymbol{K}) &= \left(\frac{\omega_1 + \omega_2}{\omega_1 \omega_2} K_1 - \frac{\omega_1}{\omega_1 \omega_2} K_2 + A_1 \right) (\xi_1 B + K_1) \\ &+ \sum_{i=2}^{N-2} \left(-\frac{\omega_{i+1}}{\omega_i \omega_{i+1}} K_{i-1} + \frac{\omega_i + \omega_{i+1}}{\omega_i \omega_{i+1}} K_i - \frac{\omega_i}{\omega_i \omega_{i+1}} K_{i+1} + A_i \right) (\xi_i B + K_i) \\ &+ \left(\frac{\omega_N + \omega_{N-1}}{\omega_N \omega_{N-1}} K_{N-1} - \frac{\omega_N}{\omega_N \omega_{N-1}} K_{N-2} + A_{N-1} \right) (\xi_{N-1} B + K_{N-1}) . \end{aligned} \tag{6.34}$$

We now simplify $G(\boldsymbol{K})$. For this, we need the following identity:

$$\begin{aligned} &- \frac{\omega_{i+1}}{\omega_i \omega_{i+1}} K_{i-1} + \frac{\omega_i + \omega_{i+1}}{\omega_i \omega_{i+1}} K_i - \frac{\omega_i}{\omega_i \omega_{i+1}} K_{i+1} + A_i \\ &= \frac{-\omega_{i+1}}{\omega_i \omega_{i+1}} (K_{i-1} + \xi_{i-1} B) + \frac{\omega_i + \omega_{i+1}}{\omega_i \omega_{i+1}} (K_i + \xi_i B) - \frac{\omega_i}{\omega_i \omega_{i+1}} (K_{i+1} + \xi_{i+1} B) \\ &+ \left[\frac{-\omega_{i+1}}{\omega_i \omega_{i+1}} \xi_{i-1} + \frac{\omega_i + \omega_{i+1}}{\omega_i \omega_{i+1}} \xi_i + \frac{-\omega_i}{\omega_i \omega_{i+1}} \xi_{i+1} \right] B. \end{aligned}$$

The sum in the square brackets is zero, because $\boldsymbol{\xi}$ solves (6.15). Thus, we have

$$\begin{aligned} &\frac{-\omega_{i+1}}{\omega_i \omega_{i+1}} K_{i-1} + \frac{\omega_i + \omega_{i+1}}{\omega_i \omega_{i+1}} K_i - \frac{\omega_i}{\omega_i \omega_{i+1}} K_{i+1} + A_i \\ &\qquad = \frac{-\omega_{i+1}}{\omega_i \omega_{i+1}} y_{i-1} + \frac{\omega_i + \omega_{i+1}}{\omega_i \omega_{i+1}} y_i - \frac{\omega_i}{\omega_i \omega_{i+1}} y_{i+1}. \end{aligned} \tag{6.35}$$

In analogy to (6.35), we also obtain

$$\frac{\omega_1 + \omega_2}{\omega_1 \omega_2} K_1 - \frac{\omega_1}{\omega_1 \omega_2} K_2 + A_1 = \frac{\omega_1 + \omega_2}{\omega_1 \omega_2} y_1 - \frac{\omega_1}{\omega_1 \omega_2} y_2, \tag{6.36}$$

$$\frac{\omega_N+\omega_{N-1}}{\omega_{N-1}\omega_N}K_{N-1}-\frac{\omega_N}{\omega_{N-1}\omega_N}K_{N-2}+A_{N-1} = \frac{\omega_N+\omega_{N-1}}{\omega_{N-1}\omega_N}y_{N-1}-\frac{\omega_N}{\omega_{N-1}\omega_N}y_{N-2}. \tag{6.37}$$

Using (6.35)–(6.37), we obtain (6.31). □

We want to show that $L(u_1,u_2,\dots,u_n)\to 0$ as $t\to\infty$. Since $L(\boldsymbol{K})$ has a unique zero at $\boldsymbol{K}=\bar{\boldsymbol{K}}$, the statement above would imply that the solution of (1.2) will approach the limit cycle, which is to leading order given by (6.17) with $\boldsymbol{K}=\bar{\boldsymbol{K}}$, provided that (6.1) holds. We also are interested in identifying the d-dependence of the rate of system's approach to the limit cycle. For this, we get the following expression for $L(\boldsymbol{K})$.

PROPOSITION 6.4.

$$L(\boldsymbol{K})\equiv Q(\boldsymbol{y},\boldsymbol{y})=\frac{1}{2}\sum_{k=1}^{N-1}\left(\Lambda_i\boldsymbol{y}\right)^2, \tag{6.38}$$

where the discrete operators Λ_i are defined as follows:

$$\Lambda_1\boldsymbol{y}=\frac{-1}{\omega_1\omega_2}\left(-(\omega_1+\omega_2)y_1+\omega_1y_2\right), \tag{6.39}$$

$$\Lambda_i\boldsymbol{y}=\frac{-1}{\omega_i\omega_{i+1}}\left(\omega_{i+1}y_{i-1}-(\omega_i+\omega_{i+1})y_i+\omega_{i-1}y_{i+1}\right), \qquad i=2,3,\dots,N-2, \tag{6.40}$$

$$\Lambda_{N-1}\boldsymbol{y}=\frac{-1}{\omega_{N-1}\omega_N}\left(-(\omega_{N-1}+\omega_N)y_{N-1}+\omega_Ny_{N-2}\right), \tag{6.41}$$

and $y_i, i=1,2,\dots,N-1$ are the same as in (6.31).

Proof. Equation (6.38) follows from (6.29) using (6.35)–(6.37). □

Note that $Q(\boldsymbol{y},\boldsymbol{y})\ge 0$ for any $\boldsymbol{y}\in\mathbb{R}^N$. Moreover, $Q(\boldsymbol{y},\boldsymbol{y})=0$ if and only if $\boldsymbol{\Lambda y}=0$, where the matrix $\boldsymbol{\Lambda}$ was defined in (6.13). Since matrix $\boldsymbol{\Lambda}$ is nonsingular, the quadratic form $Q(\boldsymbol{y},\boldsymbol{y})$ is positive definite. By standard results from linear algebra, the quadratic forms $P(\boldsymbol{y},\boldsymbol{y})$ and $Q(\boldsymbol{y},\boldsymbol{y})$ can be simultaneously reduced to canonical form by the change of basis [22], because they are positive definite.

In new coordinates,

$$P(\boldsymbol{y},\boldsymbol{y})=\eta_1^2+\eta_2^2+\cdots+\eta_{N-1}^2, \tag{6.42}$$

$$Q(\boldsymbol{y},\boldsymbol{y})=\lambda_1\eta_1^2+\lambda_2\eta_2^2+\cdots+\lambda_{N-1}\eta_{N-1}^2, \tag{6.43}$$

where all $\lambda_i(\omega_1,\omega_2,\dots,\omega_N)$ are positive, because $Q(\boldsymbol{y},\boldsymbol{y})$ is positive definite. Choosing $\underline{\lambda}=\min_i\{\lambda_i\}$ and $\bar{\lambda}=\max_i\{\lambda_i\}$, we have

$$\underline{\lambda}P(\boldsymbol{y},\boldsymbol{y})\le Q(\boldsymbol{y},\boldsymbol{y})\le\bar{\lambda}P(\boldsymbol{y},\boldsymbol{y}). \tag{6.44}$$

The combination of (6.44), (6.31), and (6.33) yields

$$-\delta\bar{\lambda}L\le\frac{\Delta L}{T}\le-\delta\underline{\lambda}L, \tag{6.45}$$

where the constants $\underline{\lambda}$ and $\bar{\lambda}$ depend on $\omega_1,\omega_2,\dots,\omega_N$. The last equation shows that the system evolves toward a stationary state of L that is the limit cycle determined to leading order by (6.17) with $\boldsymbol{K}=\bar{\boldsymbol{K}}$. Moreover, the rate of approach is proportional to $\delta\equiv\frac{1}{d}$ and is slow for strong coupling.

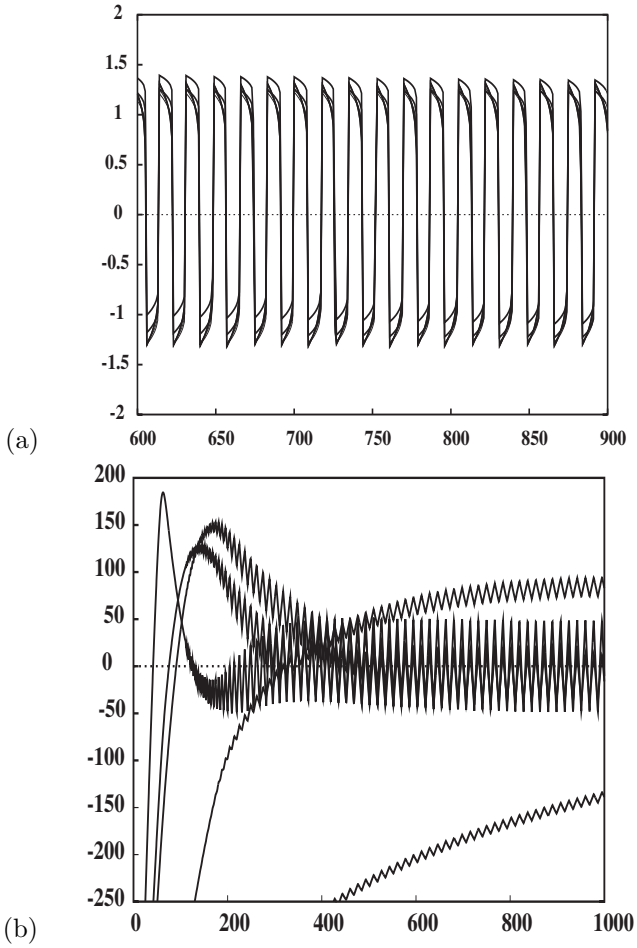

FIG. 10. *The time series plots of* (a) $v_i(t)$ *and* (b) $u_i(t)$ *for a chain of* 10 *oscillators* (1.2). *The values of parameters are* $d = 1000$, $\epsilon = 1$, $\omega_i = i$, *and* $f(x) = 4x(2 - x^4)(x^2 + 5)$. *Our choice of* $f(v)$ *for this figure is motivated by our desire to illustrate best the character of transients. The qualitative features of the system's dynamics do not depend on any particular choice of* $f(v)$. *All* v_i *variables undergo almost identical oscillations. The variables* u_i *oscillate with different amplitudes and exhibit pronounced transient dynamics. Note that though* L *decreases monotonically in time, the concentration variables* u_i *may change in a nonmonotone manner. This is explained by the fact that* L *is a function of the squared differences* $(\frac{u_i}{\omega_i} - \frac{u_{i-1}}{\omega_{i-1}})^2$.

We conclude this section by presenting a numerical example. For this, we choose a chain of 10 oscillators of the type (1.2) coupled diffusively. Figure 10(a) presents almost identical oscillations of all 10 v_i variables. Figure10(b) shows that the u_i variables undergo oscillations of different amplitudes, but all of them stay in synchrony. This plot also exhibits a well-pronounced transition period. To illustrate our conclusions about the durations of transients on Figure 11 we plot the function L in time for two different values of the strength of coupling. From the numerical data presented in Figures 10 and 11 one can see that the analytical results of this section agree well with the results of numerical simulations.

Remark 6.1. All the calculations of this section go through for chains of the FitzHugh–Nagumo oscillators with inhomogeneous coupling, i.e., for the system of

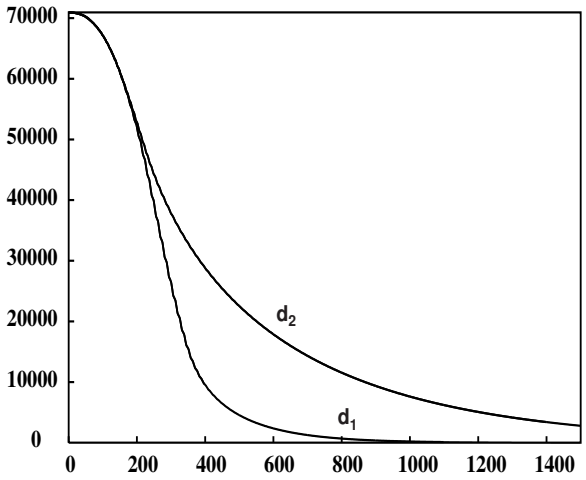

FIG. 11. *This figure presents numerically computed values of the Lyapunov function, $L(t)$, for a system of* 10 *oscillators for two different strengths of coupling $d_1 = 500$ and $d_2 = 1000$. Two exponential curves decay to* 0 *at different rates and, therefore, show the dependence of the duration of transient phase on d. The other parameters are the same as in Figure* 10.

equations (1.2) where the coupling terms $d(v_{i+1}-v_i)$ are replaced by the similar terms with positive weights: $dr_i(v_{i+1}-v_i),\ i=1,2,\dots,N-1$. To extend the analysis of this section to cover such chains it is sufficient to modify the definitions of $\boldsymbol{c}(v_1)$ and $L(\boldsymbol{u})$ as follows:

$$c_i(v_1) = dr_i(v_{i+1}-v_i),\ i=1,2,\dots,N-1,$$

$$L(\boldsymbol{u}) = \frac{1}{2}\sum_{i=1}^{N-1} r_i\left(\frac{u_{i+1}}{\omega_{i+1}} - \frac{u_i}{\omega_i}\right)^2.$$

7. Rigorous justification for the asymptotic analysis of section 6. The goal of this section is to provide a rigorous justification for the asymptotic analysis of dynamics of chains of N coupled FitzHugh–Nagumo oscillators presented in the previous section.

As before, we assume that the nonlinearity $f(v)$ in (1.2) is qualitatively "cubic," i.e., it has two extrema and

$$\lim_{x\to\pm\infty} f(x) = \mp\infty. \tag{7.1}$$

Under these assumptions we prove the following theorem.

THEOREM 7.1. *Let $D_0 \subset \mathbb{R}^{2N}$ be a bounded domain, and let $Z_{\epsilon,\delta}$ denote the phase trajectory $(\boldsymbol{v}(t),\boldsymbol{u}(t))$ of* (1.2) *with $d = \frac{1}{\delta}$ and initial data $(\boldsymbol{v}(0),\boldsymbol{u}(0)) \in D_0$. Then after time t_0, which depends on D_0 only, for sufficiently small $\epsilon > 0$ and sufficiently large d the following two statements hold:*

1. *For arbitrary $s > t_0 > 0$ let $\boldsymbol{K}_s = \boldsymbol{\Lambda}^{-1}\boldsymbol{h}(\boldsymbol{u}(s))$, where $\boldsymbol{\Lambda}$ and $\boldsymbol{h}$ are defined in* (6.13) *and* (6.18)*, respectively. The trajectory $Z_{\epsilon,\delta}$ tends to the singular trajectory $Z_{0,0}(\boldsymbol{K}_s)$ in the C^0-metric as $\epsilon \to 0$ and $\delta \to 0$ uniformly on any finite time interval $[s, s+T]$ and with respect to initial data $(\boldsymbol{v}(0),\boldsymbol{u}(0)) \in D_0$.*

2. *In addition, as* $t \to \infty$, $Z_{\epsilon,\delta}$ *approaches a closed trajectory* $Z_{0,0}(\bar{\boldsymbol{K}})$

$$Z_{\epsilon,\delta} \to Z_{0,0}(\bar{\boldsymbol{K}}),$$

where $\bar{\boldsymbol{K}}$ *is defined in* (6.30).

Remark 7.1. Note that the latter statement of the theorem implies that (1.2) possesses a globally attracting limit cycle.

To justify the matched asymptotic scheme we need to show that the ansatz

$$v_{i+1} - v_i = O(\delta), \quad i = 1, 2, \dots, N-1,$$

which we have adopted in (6.1), indeed holds. Then we can use the well-known results on singularly perturbed systems [14] to show that after some initial time the trajectories of (1.2) are $O(\epsilon + \delta)$ close to the cylinder $\boldsymbol{\gamma} = \bigcup_{\boldsymbol{K}} \boldsymbol{\gamma}(\boldsymbol{K})$, built up from the singular orbits (6.19). This accuracy is sufficient for construction of the Lyapunov function L (6.24) and for analyzing the system's dynamics on the cylinder γ.

First we formulate and prove a few auxiliary lemmas. The first two are concerned with the boundary layer behavior that takes the trajectory from the initial conditions to a neighborhood of the singular periodic orbits $\boldsymbol{\gamma}(\boldsymbol{K})$. This boundary layer occurs on two time scales. The first lemma deals with the first part, occurring at the superfast $O(d)$ speed on the fast time scale, in which the trajectory approaches the diagonal manifold $v_i \approx v_j$ for all i, j. The second lemma deals with the approach, at an $O(1)$ speed, to the cylinder $\boldsymbol{\gamma} = \bigcup_{\boldsymbol{K}} \boldsymbol{\gamma}(\boldsymbol{K})$. The next two lemmas concern dynamics near the slow manifold. The first shows that the Lyapunov function decays; with this used to constrain the possible values of L, the next lemma shows that the trajectory must stay close to a limited portion of $\boldsymbol{\gamma}$ for all (slow) time. All the above lemmas use the bootstrapping hypothesis that the trajectories stay in some bounded domain for all time. The final lemma uses estimates obtained from the first four lemmas to construct a bounded domain guaranteed to contain for all time the trajectories starting in a given bounded domain. After this Theorem 7.1 can easily be proved.

The following lemma shows that for arbitrary initial data, after some time all v_i components become $O(\delta)$ close, provided that the trajectory remains bounded and the coupling constant d is sufficiently large.

LEMMA 7.2. *Let* $D \subset \mathbb{R}^{2N}, M = diam\, D < \infty$. *Then as long as* $(\boldsymbol{v}(t), \boldsymbol{u}(t)) \in D$, *we have*

$$|v_{i+1}(t) - v_i(t)| \le \frac{C_1}{d}, \quad i = 1, 2, \dots, N-1, \tag{7.2}$$

for $t \ge t_1 \equiv \epsilon \frac{\ln(e+1)}{e+1}$, $d \ge d_0 \equiv \frac{e+1}{\lambda}$, *and* $\lambda = 4 \sin^2 \frac{\pi}{2(N+1)}$. *The constant* C_1 *does not depend on* d.

Proof. Define $\boldsymbol{z} = (z_1, z_2, \dots, z_{N-1})^T$, where $z_i = v_{i+1} - v_i, i = 1, 2, \dots, N-1$. Then by changing to the fast time variable $\tau = \frac{t}{\epsilon}$ and by subtracting the equation for v_i from the equation for v_{i+1} in (1.2) we find

$$\begin{aligned} &\frac{d\boldsymbol{z}}{d\tau} = d\Delta_0 \boldsymbol{z} + \boldsymbol{g}, \quad \boldsymbol{g} = (g_1, g_2, \dots, g_{N-1}), \quad g_i = f(v_{i+1}) - f(v_i) - u_{i+1} + u_i, \\ &\qquad i = 1, 2, \dots, N-1, \end{aligned} \tag{7.3}$$

where $\Delta_0 : \mathbb{R}^{N-1} \to \mathbb{R}^{N-1}$ denotes the second order difference operator

$$(\Delta_0 \boldsymbol{z})_i \equiv \begin{cases} z_2 - 2z_1, & i = 1, \\ z_{i+1} - 2z_i + z_{i-1}, & i = 2, 3, \dots, N-2, \\ z_{N-2} - 2z_{N-1}, & i = N-1. \end{cases}$$

It is well known that the eigenvalues of the linear operator $\Delta_0 : \mathbb{R}^{N-1} \to \mathbb{R}^{N-1}$ are all real and negative [20]. The largest eigenvalue is $-\lambda = -4\sin^2 \frac{\pi}{2(N+1)}$.

As long as $(\boldsymbol{v}(t), \boldsymbol{u}(t)) \in D$, from (7.3) we have

$$\frac{d\boldsymbol{z}}{d\tau} \le -d\lambda \boldsymbol{z} + C_2,$$

where

$$C_2 = M(l_f + 2) \quad \text{and} \quad l_f = \max_{|x| \le M+1} |f'(x)|.$$

Thus,

$$|\boldsymbol{z}(\tau)| \le 2Me^{-d\lambda\tau} + \frac{C_2}{d\lambda\tau}\left(1 - e^{-d\lambda\tau}\right) \le \frac{C_2}{d\lambda} + 2C_2 e^{-d\lambda\tau}. \tag{7.4}$$

It is easy to check that for $\tau \ge \tau_1 \equiv \frac{\ln(e+1)}{e+1}$ and $d \ge d_0 \equiv \frac{e+1}{\lambda}$

$$e^{-d\lambda\tau} \le \frac{1}{d\lambda}. \tag{7.5}$$

Inequalities (7.4) and (7.5) imply that

$$|\boldsymbol{z}| \le \frac{3C_2}{\lambda}\frac{1}{d}, \quad t \ge \epsilon\tau_1 \equiv t_1, d \ge d_0, \tag{7.6}$$

and provided that $(\boldsymbol{v}(t), \boldsymbol{u}(t)) \in D$. This proves (7.2). □

In the next lemma we will show that under the assumptions of Lemma 7.2 the trajectory $Z_{\epsilon,\delta}$ stays $O(\epsilon + \delta)$ close in C^0-metric to $\boldsymbol{\gamma}$. Recall that we have defined $\boldsymbol{\gamma}$ as a union of singular periodic orbits (6.19) $\boldsymbol{\gamma}(\boldsymbol{K}) = (\gamma_1 \times \gamma_2 \times \cdots \times \gamma_N)(\boldsymbol{K})$ over all $\boldsymbol{K} \in \mathbb{R}^{N-1}$.

LEMMA 7.3. *Let $D \in \mathbb{R}^{2N}$, diam $D = M < \infty$. Then there exists $t_0 > 0$ such that for any $T_1 > 0$ there exist $\epsilon_0 > 0$ and $\delta_0 > 0$ such that for all $\epsilon < \epsilon_0$ and $d > \frac{1}{\delta_0}$ any trajectory $(\boldsymbol{v}(t), \boldsymbol{u}(t))$ of (1.2) with initial data from D satisfies*

$$dist\left((\boldsymbol{v}(t), \boldsymbol{u}(t)), \boldsymbol{\gamma}(\boldsymbol{K}_s)\right) \le C_3(\epsilon + \delta), \quad s \le t \le s + T_1, s \ge t_0, \tag{7.7}$$

provided $(\boldsymbol{v}(t), \boldsymbol{u}(t))$ remains in D. The positive constant C_3 depends on T_1, but not on ϵ or δ.

Proof. Recall that after the time t_1, defined in Lemma 7.2, (7.2) is guaranteed to hold. Let $s > t_1$ be a fixed moment of time. By $Z_{\epsilon,\delta}$ we denote the trajectory of (1.2) with initial condition $(\boldsymbol{v}^0, \boldsymbol{u}^0) \equiv (\boldsymbol{v}(s), \boldsymbol{u}(s)) \in D$. We suppose that $Z_{\epsilon,\delta} \in D$ for the interval of time under consideration. Following the standard procedure in singular perturbations theory [14], we construct a singular $(\epsilon = 0, \delta = 0)$ trajectory $Z_{0,0}(\boldsymbol{K}_s)$ (cf. Definition 6.2).

We also consider a singular trajectory $Z_{0,\delta}$, the slow dynamics of which are defined by the degenerate system (6.5), (6.6) with initial condition $(\boldsymbol{v}^0, \boldsymbol{u}^0)$ and with function $\boldsymbol{c}(v_1)$ satisfying (6.13). We now show that $Z_{0,\delta}$ is well defined and is a regular perturbation of $Z_{0,0}(\boldsymbol{K}_s)$. For this, it is sufficient to show that $\|\boldsymbol{\sigma}(v_1)\|$ in (6.13) is bounded in D as $\delta \to 0$. $\boldsymbol{\sigma}(v_1)$ depends on $f(v_1), f'(v_1), f''(v_1), v_1, \boldsymbol{c}(v_1)$, and $\boldsymbol{c}'(v_1)$. Functions $f(v_1), f'(v_1), f''(v_1)$ are continuous for $(\boldsymbol{v}, \boldsymbol{u}) \in D$ and, therefore, are bounded, as is

$\boldsymbol{c}(v_1)$ by Lemma 7.2. A bound on $\|\boldsymbol{c}'(v_1)\|$ can be obtained from (6.13) by a bootstrapping argument: It is straightforward to check that $\boldsymbol{\sigma}(v_1)$ contains only terms linear in $\boldsymbol{c}'(v_1)$. Therefore, (6.13) can be rewritten as

$$(\boldsymbol{\Lambda} + \delta \boldsymbol{E})\, \boldsymbol{c}' = f' \boldsymbol{\theta} + \delta \hat{\boldsymbol{\sigma}}(v_1), \tag{7.8}$$

where all terms containing c' are now taken to the left-hand side and $\hat{\boldsymbol{\sigma}}$ depends on f, f', f'', and $\boldsymbol{c}$. The entries of an $(N-1) \times (N-1)$ matrix $\boldsymbol{E}$ are bounded in D. We conclude that $\|\boldsymbol{c}'(v_1)\|$ is bounded in D, because the right-hand side of (7.8) is bounded, and the matrix $(\boldsymbol{\Lambda} + \delta \boldsymbol{E})$ is invertible for small δ. Therefore, $Z_{0,\delta} \to Z_{0,0}(\boldsymbol{K}_s)$, as $\delta \to 0$.

Geometrically, we construct $Z_{0,\delta}$ as follows. Define the surface $\boldsymbol{\Gamma}_\delta(K_s)$, on which $\frac{d\boldsymbol{v}}{dt} = 0$ to leading order in δ, i.e.,

$$\boldsymbol{\Gamma}_\delta(\boldsymbol{K}_s) = \{(\boldsymbol{v}, \boldsymbol{u}) \in \mathbb{R}^{2N} | \boldsymbol{u} = \boldsymbol{f}(v_1) + \boldsymbol{S}\boldsymbol{c}(v_1) + \delta \boldsymbol{\mu}(v_1), \;\; v = v_1\}.$$

As we have shown in the previous paragraph, the slow manifolds $\boldsymbol{\Gamma}_\delta(\boldsymbol{K}_s)$ and $\boldsymbol{\Gamma}(\boldsymbol{K}_s)$ are C^1 close for small $\delta > 0$. Therefore, the slow manifold $\boldsymbol{\Gamma}_\delta(\boldsymbol{K}_s)$ and its boundaries are well defined and are regular perturbations of $\boldsymbol{\Gamma}(\boldsymbol{K}_s)$. We next define a singular trajectory $Z_{0,\delta}(\boldsymbol{K}_s)$ for (1.2) as an alternating sequence of fast jumps and the slow motions along the stable branches of $\boldsymbol{\Gamma}_\delta(\boldsymbol{K}_s)$. For such trajectory $Z_{0,\delta}(\boldsymbol{K}_s)$ and for any finite time $T_2 > 0$ (T_2 will be specified below) we have

$$|Z_{0,\delta}(\boldsymbol{K}_s) - Z_{0,0}(\boldsymbol{K}_s)| \le C_4 \delta, \quad s \le t \le s + T_2, \;\; \delta \le \delta_0, \tag{7.9}$$

because $Z_{0,\delta}(\boldsymbol{K}_s)$ is a regular perturbation of $Z_{0,0}(\boldsymbol{K}_s)$.

On the other hand, from the results of singular perturbations theory [14] we know that in a bounded region of phase space, $Z_{0,\delta}(\boldsymbol{K}_s)$ provides a zeroth order approximation of $Z_{\epsilon,\delta}$, i.e., $Z_{\epsilon,\delta} \to Z_{0,\delta}(\boldsymbol{K}_s)$ as $\epsilon \to 0$ uniformly on any bounded interval of time. In particular, for $\epsilon > 0$ sufficiently small we have

$$|Z_{0,\delta}(\boldsymbol{K}_s) - Z_{\epsilon,\delta}| < C_5 \epsilon, \quad s \le t \le s + T_2. \tag{7.10}$$

The combination of (7.9) and (7.10) yields that $Z_{\epsilon,\delta} \to Z_{0,0}(\boldsymbol{K}_s)$ as $\epsilon \to 0$ and $\delta \to 0$ uniformly on any finite interval of time $s \le t \le s + T_2$ and with respect to initial conditions $(\boldsymbol{v}^0, \boldsymbol{u}^0) \in D$.

The estimates above and the definition of the singular trajectory $Z_{0,0}(\boldsymbol{K}_s)$ imply that for $t_1 \le t \le t_1 + T_2$ the phase point $(\boldsymbol{v}(t), \boldsymbol{u}(t))$ stays in an $O(\epsilon + \delta)$ neighborhood of the singular ($\epsilon = \delta = 0$) orbit consisting of fast jumps and slow motions along the stable branches of $\boldsymbol{\Gamma}(\boldsymbol{K}_s)$. Then if the phase point has not already reached the generalized nullcline (as in the situation depicted in Figure 12), it will move first along the line AB (see Figure 12) until it reaches the neighborhood of the generalized nullcline in the vicinity of point B. This part of the motion is taking place on the fast, i.e., $O\left(\frac{1}{\epsilon}\right)$, time scale. After this, the phase point will move upward along the generalized nullcline and will enter the neighborhood of the periodic orbit $\boldsymbol{\gamma}(\boldsymbol{K})$ near C. The time of this part of motion is $O(1)$. The combined time of the motion from A to B and from B to C is estimated by t_2. Therefore, after time $t_1 + t_2$ the phase point is guaranteed to be in a neighborhood of the cylinder $\boldsymbol{\gamma}$ and it will stay there, as long as $(\boldsymbol{v}(t), \boldsymbol{u}(t)) \in D$. Let $T_2 = T_1 + t_2$, $t_0 \equiv t_1 + t_2$. With these definitions of t_0 and T_2 (7.7) holds. □

We have shown so far, that after initial time t_0 and as long as $(\boldsymbol{v}(t), \boldsymbol{u}(t)) \in D$, the trajectories that have started from $D^0 \subset \mathbb{R}^{2N}$ have all v_i components $O(\delta)$ close

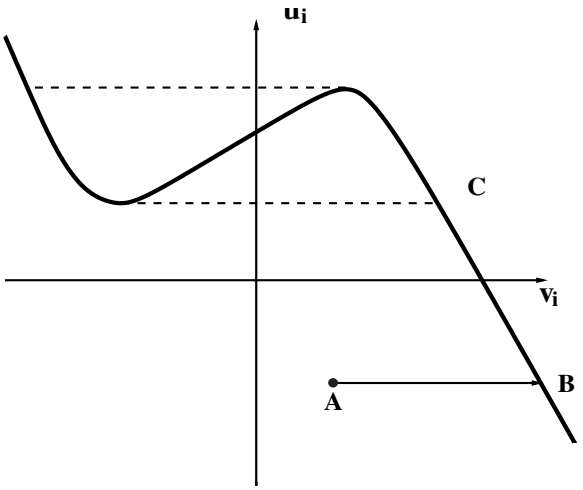

FIG. 12. *This figure illustrates schematically the estimates of the Lemma* 7.3. *See the proof of Lemma* 7.3 *for comments.*

to each other and undergo relaxation oscillations. The leading order approximation of the period follows directly from Lemma 7.3 and the well-known results for the relaxation oscillations (Chapter III in [14]). In particular, we have the following corollary.

COROLLARY 7.4. *Under the assumptions of Lemma* 7.3*, after time* t_0*, the period* $T_{\epsilon,\delta}$ *of relaxation oscillations of the coupled system* (1.2) *is equal to*

$$T_{\epsilon,\delta} = T^0 + O(\epsilon + \delta), \tag{7.11}$$

where T^0 *is given in* (6.22).

Another useful implication of Lemma 7.3 is as follows.

COROLLARY 7.5. *Under the assumptions of Lemma* 7.3*,*

$$dist\left((\boldsymbol{v}(t), \boldsymbol{u}(t)), \gamma\right) < C_6(\epsilon + \delta), \quad \boldsymbol{\gamma} \equiv \bigcup_{\boldsymbol{K}} \boldsymbol{\gamma}(\boldsymbol{K}), \quad t \geq t_0, \tag{7.12}$$

where the constant C_6 *is independent of* ϵ *and* δ.

Proof. Apply the argument of the proof of Lemma 7.3 for each time interval $[nT_2, (n+1)T_2]$, $n \in \mathbb{N}$. □

To study the evolution of the system on the infinite cylinder $\boldsymbol{\gamma}$ we have employed the Lyapunov function L (6.24). In the following lemma, we show that L decays exponentially on solutions of (1.2) provided that the solutions are uniformly bounded.

LEMMA 7.6. *There exists* $\bar{t}(\delta) > 0$ *such that*

$$|L(t)| \leq C_7\left(\epsilon + \delta\right) \quad \textit{for} \quad t > \bar{t}(\delta) \tag{7.13}$$

and as long as $(\boldsymbol{v}(t), \boldsymbol{u}(t)) \in D$.

Proof. Let T^0 be the leading order approximation of the period of relaxation oscillations of the coupled system given in (6.22). Lemma 7.3 implies that for sufficiently small positive ϵ and δ there exists $\boldsymbol{K}_{t'} \in \mathbb{R}^{N-1}$ such that

$$\text{dist}\left((\boldsymbol{v}(t), \boldsymbol{u}(t)), \boldsymbol{\gamma}(\boldsymbol{K}_{t'})\right) \leq C_8(\epsilon + \delta), \quad t_0 < t' \leq t \leq t' + T_0 + 1, \tag{7.14}$$

where the singular orbit $\boldsymbol{\gamma}(\boldsymbol{K}_{t'})$ is constructed by (6.17)–(6.18). Thus, during one period $(\boldsymbol{v}(t), \boldsymbol{u}(t))$ can be approximated by $\boldsymbol{\gamma}(\boldsymbol{K}_{t'})$ with $O(\epsilon+\delta)$ accuracy.

By taking into account (7.11) and (7.14) and tracking the order of the error in the derivation of the asymptotic formula (6.32), we obtain

$$-\delta\bar{\lambda}L(t) - C_9\delta\,(\epsilon+\delta) \le \frac{\Delta L(t)}{T^0} \le -\delta\underline{\lambda}L(t) + C_{10}\delta\,(\epsilon+\delta) \tag{7.15}$$

for $t \ge t_0$ and as long as $(\boldsymbol{v}(t), \boldsymbol{u}(t)) \in D$, where $L(t) = L(\boldsymbol{u}(t))$ and $\Delta L(t) = L(t+T^0) - L(t)$. The constants C_9 and C_{10} do not depend on ϵ and δ.

From (7.15), for $t' \in [t_0, t_0+T^0]$ and $n \in \mathbb{N}$ we have

$$L_n^- \le L(t'+nT) \le L_n^+, \tag{7.16}$$

where the sequences $\{L_k^\pm\}$ are generated from $L_0^\pm = L(t')$ by the linear maps

$$L_{k+1}^+ = -\delta\underline{\lambda}L_k^+ + C_9\delta\,(\epsilon+\delta) \quad \text{and} \quad L_{k+1}^- = -\delta\bar{\lambda}L_k^- - C_{10}\delta\,(\epsilon+\delta)\,.$$

The statement of Lemma 7.6 follows from (7.16) and asymptotic behavior of $\{L_k^\pm\}$. □

In Corollary 7.5 we have shown that after some time $t \ge t_0$, $Z_{\epsilon,\delta}$ stays in some $O(\epsilon+\delta)$ neighborhood of the *infinite* cylinder $\boldsymbol{\gamma} = \bigcup_{\boldsymbol{K}} \boldsymbol{\gamma}(\boldsymbol{K})$. By Lemma 7.6 the function L evaluated on $Z_{\epsilon,\delta}$ eventually decays to zero and therefore is bounded. In the next lemma we use the bound on L to restrict the dynamics of $Z_{\epsilon,\delta}$ to the neighborhood of a *finite* cylinder.

LEMMA 7.7. *Suppose the trajectory $Z_{\epsilon,\delta}$ of (1.2) is contained in a bounded domain D. If the function L evaluated on $Z_{\epsilon,\delta}$ is bounded,*

$$|L| \le \bar{L}, t \ge t_0, \tag{7.17}$$

then after $t = t_0$, $Z_{\epsilon,\delta}$ stays in the $O(\epsilon+\delta)$ vicinity of the finite cylinder

$$\boldsymbol{\gamma}(\mathcal{K}_{\bar{L}}) = \bigcup_{\boldsymbol{K}\in\mathcal{K}_{\bar{L}}} \boldsymbol{\gamma}(\boldsymbol{K}), \quad \mathcal{K}_{\bar{L}} = \{\boldsymbol{K} : |\boldsymbol{K} + B\boldsymbol{\xi}| \le \left|\Lambda^{-1}\right| \sqrt{2\bar{L}}\} \tag{7.18}$$

for sufficiently small $\epsilon > 0$ and $\delta > 0$.

Proof. Since $Z_{\epsilon,\delta}$ can be approximated to leading order in ϵ and δ by a singular orbit $Z_{0,0}(\boldsymbol{K})$ it follows from the derivation of (6.38) that the Lyapunov function $L(\boldsymbol{u})$ can be in turn approximated by the quadratic form $L(\boldsymbol{K}) \equiv Q(\boldsymbol{y},\boldsymbol{y})$: $L(\boldsymbol{u}) = Q(\boldsymbol{y},\boldsymbol{y}) + O(\epsilon+\delta)$. Using the assumption (7.17), for sufficiently small $\epsilon > 0$ and $\delta > 0$ we get

$$L(\boldsymbol{K}) = \frac{1}{2}\sum_{i=1}^{N-1} (\Lambda_i \boldsymbol{y})^2 = \frac{1}{2}\left(l_1^2 + l_2^2 + \cdots + l_N^2\right) \le \bar{L} + C_{11}(\epsilon+\delta), \tag{7.19}$$

where $l_i \equiv \Lambda_i \boldsymbol{y}$, $i = 1, 2, \ldots, N-1$. Consequently,

$$\Lambda_i \boldsymbol{y} = \Lambda_i\,(\boldsymbol{K} + B\boldsymbol{\xi}) = l_i, \quad |l_i| \le \sqrt{2\bar{L}} + C_{12}(\epsilon+\delta), \quad i = 1, 2, \ldots, N,$$

where the bound for $|l_i|$ follows from (7.19). Rewriting the last equation in matrix form, we have

$$\Lambda\,(\boldsymbol{K} + B\boldsymbol{\xi}) = l, \tag{7.20}$$

where $\mathbf{\Lambda}$ is defined in (6.39)–(6.44). Since $\mathbf{\Lambda}$ is nonsingular, we obtain the desired bound for $\boldsymbol{K}$:

$$|\boldsymbol{K} + B\boldsymbol{\xi}| = \left|\mathbf{\Lambda}^{-1} l\right| \leq \left|\mathbf{\Lambda}^{-1}\right| \left(\sqrt{2\bar{L}} + C_{12}\left(\epsilon + \delta\right)\right). \qquad \square \tag{7.21}$$

COROLLARY 7.8. *For $t \geq \bar{t}(\delta)$ and as long as $Z_{\epsilon,\delta} \in D$, the trajectory $Z_{\epsilon,\delta}$ stays in an $O(\epsilon+\delta)$ neighborhood of*

$$\boldsymbol{\gamma}(\mathcal{K}_\delta) = \bigcup_{\boldsymbol{K}\in\mathcal{K}_\delta} \boldsymbol{\gamma}(\boldsymbol{K}), \quad \mathcal{K}_\delta = \left\{\boldsymbol{K} : |\boldsymbol{K} + B\boldsymbol{\xi}| \leq C_{13}\left|\mathbf{\Lambda}^{-1}\right|\sqrt{\epsilon+\delta}\right\}$$

for $\epsilon > 0$ and $\delta > 0$ sufficiently small.

Proof. Apply Lemma 7.7 using the bound on L from Lemma 7.6. $\square$

We use now the results of the four preceding lemmas to construct a trapping region for $Z_{\epsilon,\delta}$. After this the statements of Theorem 7.1 follow directly from Lemma 7.3 and Corollary 7.8.

LEMMA 7.9. *Let $D_0 \subset \mathbb{R}^{2N}$ be a bounded domain. There exists a bounded domain $D_2 \subset \mathbb{R}^{2N}$ such that the trajectory $Z_{\epsilon,\delta}$ with initial data from D_0 does not leave D_2.*

Proof. First we note that for any finite time $T > 0$ there exists a bounded domain $D_T \subset \mathbb{R}^{2N}$ such that

$$Z_{\epsilon,\delta} \in D_T, \quad 0 \leq t \leq T.$$

We now show that, for sufficiently small ϵ and δ, the size of D_T does not depend on either of them. For a singularly perturbed system (1.2) one can separate the system dynamics into two parts: slow motions and fast jumps (see [14] for details). Without loss of generality, we can assume that during the interval of time under consideration the jump is followed by slow motion. During the jump the change of the slow variable $\boldsymbol{u}$ is $O(\epsilon)$. Thus, for ϵ sufficiently small $\boldsymbol{u}$ stays bounded during the fast jump, e.g., $|\boldsymbol{u}| \leq 2M$, $M = \mathrm{diam} D_0$. To find the corresponding bound for $\boldsymbol{v}$ we consider

$$\begin{aligned} \frac{d}{dt}\frac{1}{2}\sum_{i=1}^{N} v_i^2 &= \frac{1}{\epsilon}\left(\sum_{i=1}^{N}\left(f(v_i) - u_i\right)v_i - d\sum_{i=1}^{N-1}\left(v_{i+1} - v_i\right)^2\right) \\ &\leq \frac{1}{\epsilon}\sum_{i=1}^{N}\left(f(v_i) - u_i\right). \end{aligned} \tag{7.22}$$

Using (7.1) and the bound for $\boldsymbol{u}$, from (7.22) one can obtain the bound for $\boldsymbol{v}$.

During the slow motions the time derivatives $\frac{du_i}{dt}$ and $\frac{dv_i}{dt}$ are $O(1)$ and the trajectories of (1.2) with initial data from the bounded domain D_0 remain bounded for finite interval of time according to Gronwall's inequality.

We need to make several auxiliary definitions. By D_{t_0+1} we denote a bounded domain that contains $Z_{\epsilon,\delta}$ for $0 \leq t \leq t_0 + 1$. The finite cylinder $\boldsymbol{\gamma}(\mathcal{K}_{\bar{L}})$ is defined in (7.18) with $\bar{L} \equiv \max_{(\boldsymbol{v},\boldsymbol{u})\in D_{t_0+1}} |L(u)|$. The domains D_{t_0+1} and $\boldsymbol{\gamma}(\mathcal{K}_{\bar{L}})$ are bounded and, therefore, can be enclosed in the ball $B(r)$ of radius r and centered at the origin. Finally, we define a bounded domain $D_2 \equiv B(r+1)$ and D_{2,T_0} such that

$$Z_{\epsilon,\delta} \in D_2 \quad \text{at} \quad t = s \Rightarrow Z_{\epsilon,\delta} \in D_{2,T^0}, \quad s \leq t \leq s + T^0.$$

We claim that for sufficiently small $\epsilon > 0$ and $\delta > 0$ $Z_{\epsilon,\delta}$ stays in D_2 provided $(\boldsymbol{v}(0), \boldsymbol{u}(0)) \in D_0$. First, we note that

$$(\boldsymbol{v}(0), \boldsymbol{u}(0)) \in D_0 \Rightarrow Z_{\epsilon,\delta} \in D_{t_0+1} \subset D_2 \subset D_{2,T^0} \quad \text{for} \quad 0 \le t \le t_0.$$

Since $Z_{\epsilon,\delta} \in D_2$ at $t = t_0$ it is guaranteed to stay in D_{2,T^0} for the next period T^0. Therefore, by Lemma 7.7 $Z_{\epsilon,\delta}$ will be in the neighborhood of $\boldsymbol{\gamma}(\mathcal{K}_{\bar{L}})$, i.e., for sufficiently small $\epsilon > 0$ and $\delta > 0$

$$Z_{\epsilon,\delta} \in D_2 \quad \text{for} \quad t_0 \le t \le t_0 + T^0.$$

By repeating the same argument for each subsequent period T^0 we conclude that $Z_{\epsilon,\delta}$ stays forever in D_2. This proves the lemma. □

Once we know that $Z_{\epsilon,\delta}$ is uniformly bounded, it follows from Lemma 7.3 that after time t_0 $Z_{\epsilon,\delta}$ undergoes relaxation oscillations and on any finite interval of time (independent of d) it can be approximated by a singular orbit $Z_{0,0}(\boldsymbol{K}_s)$, i.e.,

$$Z_{\epsilon,\delta} \to Z_{0,0}(\boldsymbol{K}_s), \quad \boldsymbol{K}_s = \boldsymbol{\Lambda}^{-1}\boldsymbol{h}\left(\boldsymbol{u}(s)\right), \quad s \le t \le s + T, \quad \text{as} \quad \epsilon, \delta \to 0.$$

Moreover, by Lemma 7.6 $Z_{\epsilon,\delta}$ eventually gets trapped in the neighborhood of the singular orbit $Z_{0,0}(\bar{\boldsymbol{K}})$, i.e.,

$$Z_{\epsilon,\delta} \to Z_{0,0}(\bar{\boldsymbol{K}}) \quad \text{as} \quad \epsilon, \delta \to 0 \quad \text{and} \quad t \to \infty.$$

Thus, Theorem 7.1 is proved. □

8. Nullcline configuration and the dynamics of the coupled system. It is a common intuition that the form of u-nullcline does not affect the qualitative dynamics of a relaxation oscillator as long as it intersects the v-nullcline in the segment connecting two extrema. By contrast, in the current case we now show that the form of the u-nullcline plays an important role in the question of whether or not the trajectory of the coupled system converges to a limit cycle and in determining the rate of convergence.

In the previous sections we have studied the systems of oscillators with nullclines for each uncoupled oscillator vertical in the $v_i - u_i$ phase plane, i.e., the rate of change of u_i does not depend on u_i itself:

$$\frac{du_i}{dt} = \omega_i v_i. \tag{8.1}$$

The equation for u_i in the FitzHugh–Nagumo system of equations sometimes is written more generally as

$$\frac{du_i}{dt} = \omega_i \left(v_i - \kappa u_i\right). \tag{8.2}$$

In most cases κ is a small number and it is natural to expect that the dynamics of the coupled system (1.2) do not change qualitatively when the equations for $\frac{du_i}{dt}$ are substituted by (8.2). Below we shall see that the dynamics of the coupled system with the u_i-equations in the form of (8.2) depend in a subtle way on the magnitude of κ.

For simplicity of presentation, in this section we study chains of two oscillators. All conclusions hold for chains of N oscillators as well. We are interested in understanding the dynamics of two coupled FitzHugh–Nagumo oscillators:

$$\epsilon\frac{dv_i}{dt} = f(v_i) - u_i + d(v_j - v_i), \quad i = 1,2,\ j = 3-i, \tag{8.3}$$
$$\frac{du_i}{dt} = \omega_i\,(v_i - \kappa u_i)\,,$$

where $|\kappa| \ll 1$, and otherwise the notation is the same as in section 6.

Repeating the same steps as in section 2 we arrive at the counterpart of equation (3.10) with $\delta = 0$:

$$\frac{f'(v_1) + c'(v_1)}{f'(v_1) - c'(v_1)} = \frac{\omega_1\,(v_1 - \kappa u_1)}{\omega_2\,(v_1 - \kappa u_2)}. \tag{8.4}$$

The ratio on the right-hand side of (8.4) can be approximated by $\frac{\omega_1}{\omega_2}$ as in section 2, because κ is very small. Therefore, to leading order the dynamics of (8.3) is identical to that of (3.3). In particular, to leading order the phase trajectory consists of fast jumps and slow motions along the stable branches of the generalized nullclines $\Gamma_{1,2}(K)$ defined in (4.2).

A family of periodic orbits $\gamma_\kappa(K)$ constructed from $\Gamma_i(K)$ form an infinite cylinder in the phase space. To estimate the slow evolution of the phase point along this cylinder we use the function $L(u_1, u_2)$ defined in (5.1). As in section 5,

$$L(K) \geq 0 \quad \text{and} \quad L(K) = 0 \quad \text{iff} \quad K = \bar{K}, \tag{8.5}$$

where $\bar{K}$ is defined in (5.2). Moreover, (5.3) still holds. Using (3.5), (3.6), and (8.3) the second term on the right-hand side of (5.3) can be rewritten as

$$\omega_1^{-1}\frac{du_1}{dt} - \omega_2^{-1}\frac{du_2}{dt} = (v_1 - v_2) - \kappa\,(u_1 - u_2) = -c(v_1)(\delta + 2\kappa). \tag{8.6}$$

Plugging (8.6) into (5.3) and continuing along the lines of section 5, we find the analogue of (5.8), namely,

$$\frac{\Delta L}{T} = -\lambda\,(\delta + 2\kappa)\,L, \quad \lambda = \frac{2\omega_1\omega_2}{\omega_1 + \omega_2}. \tag{8.7}$$

From (8.7) we conclude that if $|\kappa| \ll \frac{\delta}{2}$, the phase trajectory will asymptotically approach the limit cycle $\gamma_\kappa\left(\bar{K}\right)$. As before, the rate of this approach is $O(\delta)$. However, if $\kappa \gg \frac{\delta}{2}$ the rate will be determined by κ (Figure 13(a)). Figures 3(c) and 13(a) exhibit different densities of the trajectories on the cylinder for $\kappa = 0$ and $\kappa = 0.02$ ($\delta = 0.01$). This reflects the fact that the rate of convergence to the limit cycle in the latter case is faster than that for the former case. Furthermore, if $\kappa < \frac{-\delta}{2}$ the trajectory will not converge to a limit cycle, but rather will spiral away until it leaves the region of validity of the asymptotic calculations (Figure 13(b)). Thus, at $\kappa = \frac{-\delta}{2}$ a bifurcation occurs. In fact, for $\kappa = -0.00485 \approx \frac{-\delta}{2}$ we find numerically that the phase trajectory does not deviate much from its initial position on the cylinder (Figure 13c).

9. Discussion. The analysis in this paper was motivated by experiments and simulations concerning the firing patterns in dopaminergic cells in the substantia nigra [30]. The experimental data suggest that compartments of the dendrites can be modeled by relaxation oscillators with different natural frequencies strongly coupled through fast variables. These assumptions led to the model (1.1). The simulations of

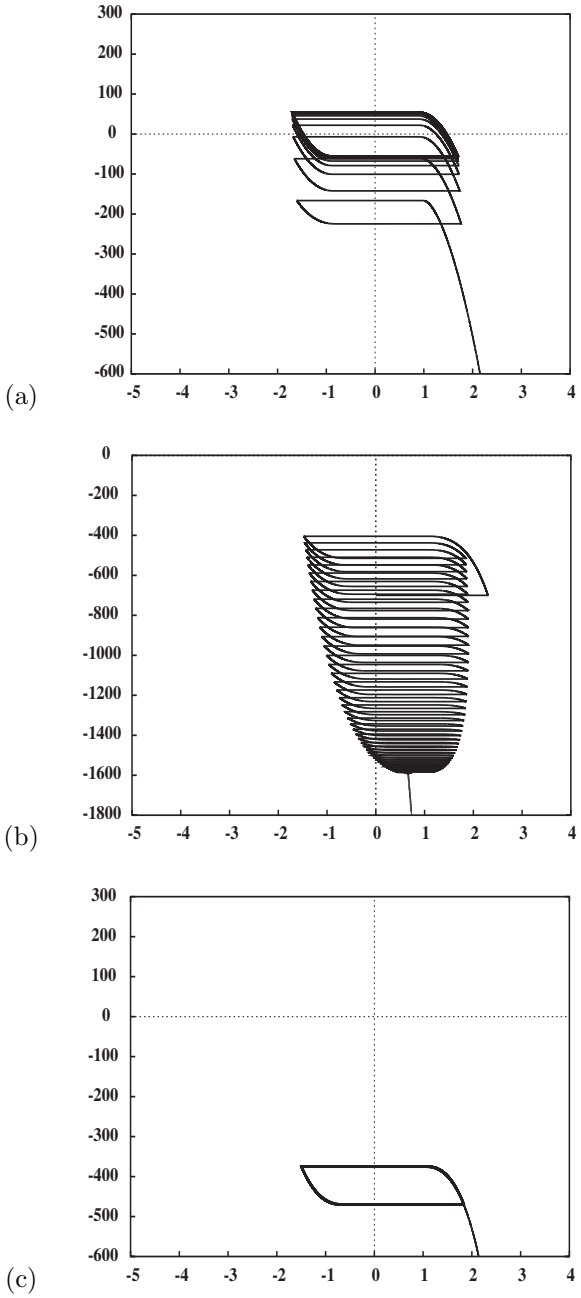

FIG. 13. *This figure presents the phase plane plots* (v_1, u_1) *for* (8.3) *with* $\delta = 0.001$ *and different values of* κ *given below. The values of the other parameters are the same as in Figure* 5. *The initial data are* $u_1 = u_2 = 700$ *and* $v_1 = v_2 = 0$, *and the time of integration is the same for all three plots.* (a) $\kappa = 0.002$. *The rate of convergence to the limit cycle is faster than that for* $\kappa = 0$. *This can be seen by comparing the density of the trajectory shown on this figure with that on Figure* 3(c). (b) $\kappa = -0.00075 < -\frac{\delta}{2}$. *The trajectory does not converge to the limit cycle but instead spirals down until the periodic solution disappears. This happens when the magnitudes of* $u_{1,2}$ *grow to* $O(d)$, $d = 1000$. *In this range the results of our asymptotic analysis are not expected to hold.* (c) $\kappa = -0.00042 \approx \frac{-\delta}{2}$. *This plot illustrates the dynamics of the coupled system near the bifurcation at* $\kappa = \frac{-\delta}{2}$. *The trajectory almost does not drift along the cylinder (compare with plots* (a) *and* (b)*). Its position is determined by the initial data.*

(1.1) showed synchronous oscillations and pronounced transient dynamics. Both the synchronous oscillations and the transients are clearly seen in the experimental data, too. Analytical understanding of these dynamical patterns was the main motivation of our work.

The analysis of the model problems (1.2) and (8.1) show a way of studying the dynamics of the physiological model based on (1.1). As the results of section 8 clearly demonstrate, the applicability of our method depends on some rather specific features of the phase planes of the individual oscillators. However, we think that the analysis for the compartmental model with kinetics given by (1.1) in the physiologically relevant range of parameteres can be performed with some modifications along the lines of analyses for (1.2) and (8.1). Without going into detail, we would like to indicate some analogies between these systems. Clearly, when the coupling is very strong the variables v_i in the coupled system for (1.1) are going to be close, like those in (1.2). Thus, the asymptotic ansatz (1.4) can be used to obtain the leading order equation for the coupling currents $c_i(v_1)$. The effective solution of the leading order problem will require a condition similar to that of the smallness of κ in (8.1). In (1.1) τ_{Ca}^{-1} plays the role of κ. If τ_{Ca}^{-1} is sufficiently small, then the equations for u_i in (1.1) effectively do not depend on u_i, like the equations for u_i in (1.2) and (8.1). This suggests that the analysis and conclusions of section 8 are relevant for the physiological model (1.1). In particular, the smallness of τ_{Ca}^{-1} is necessary for the existence of long transients seen in the simulations of (1.1). It turns out that in the physiological model the value of τ_{Ca}^{-1} is very small. Therefore, the presence of the transients in the numerical experiments for the chains of oscillators of type (1.1) (Figure 2(b)) is consistent with our conclusions for the model problems (1.1) and (8.1).

For a system of two coupled oscillators, we have developed two methods of analysis based on asymptotic expansions of solutions and on Lyapunov's method, respectively. Both methods provide a detailed description of the system's dynamics. The second method can also be used to study chains with an arbitrary number of oscillators. Our analysis reveals an unexpected structure of the phase space: in the limit of large coupling, there is an invariant manifold foliated by periodic orbits. This structure determines the behavior of solutions when the coupling is large but finite. In particular, this analysis shows an unintuitive feature of the dynamics of these systems: the transients are longer for strong coupling. We show that this is not a general property of strongly coupled relaxation oscillators, but it requires a special structure of the phase planes of individual oscillators.

There is a large body of mathematical literature related to various aspects of the current work. Individual and coupled relaxation oscillators have been studied by, e.g., Belair and Holmes [3], Storti and Rand [26], Grasman [7, 8], Rand and Holmes [17], Rubin and Terman [19], Izhikevitch [10], Wang and Rinzel [28], and Wang and Terman [29]. The effects of strong coupling on synchronization have been addressed in [1, 2, 9]. However, our major result, about the appearance of long transients in the presence of large coupling, has not been previously announced. Chains of phaselocked oscillators have been studied in the context of biological waves (Cohen, Holmes, and Rand [4], Ermentrout and Kopell [6], Kopell and Ermentrout [12], Skinner, Kopell, and Mulloney [23], and Ermentrout [5]). It has been shown that chains of relaxation oscillators have different synchronization properties than those of phase-coupled or weakly coupled oscillators and are more likely to synchronize (Somers and Kopell [24, 25], Wang [27]), even if there are differences in frequency among the oscillators, such as a frequency gradient. Indeed, chains of relaxation oscillators have been shown

to be able to synchronize very quickly compared to phase-coupled oscillators (Somers and Kopell [24], Wang [27]). Thus, it is especially surprising that the chains studied in this paper have very long transients.

Acknowledgments. We wish to thank C. J. Wilson and J. C. Callaway for introducing us to this problem, for providing the results of their experimental work and simulations, and for their help in guiding the work. We also thank T. J. Kaper and G. Osipov for useful conversations.

REFERENCES

[1] V. S. Afraimovich, N. N. Verichev, and M. I. Rabinovich, *Stochastic synchronization of oscillations in dissipative systems*, Sov. Radiophys., 29 (1986), pp. 795–800.
[2] V. S. Afraimovich, S.-N. Chow, and J. K. Hale, *Synchronization in lattices of coupled oscillators*, Phys. D, 103 (1997), pp. 442–451.
[3] J. Belair and P. Holmes, *On linearly coupled relaxation oscillators*, Quart. Appl. Math., 42 (1984), pp. 193–219
[4] A. H. Cohen, P. J. Holmes, and R. H. Rand, *The nature of the coupling between segmental oscillators of the lamprey spinal generator for locomotion: A mathematical model*, J. Math. Biol., 13 (1982), pp. 345–369.
[5] G. B. Ermentrout, J. Flores, and A. Gelperin, *Minimal model of oscillations and waves in the Limax olfactory lobe with tests of the model's predictive powers*, J. Neurophysiol., 79 (1998), pp. 2677–2689.
[6] G. B. Ermentrout and N. Kopell, *Frequency plateaus in a chain of weakly coupled oscillators* I, SIAM J. Math. Anal., 15 (1984), pp. 215–237.
[7] J. Grasman, *The mathematical modeling of entrained biological oscillators*, Bull. Math. Biol., 46 (1984), pp. 407–422.
[8] J. Grasman, *Asymptotic Methods for Relaxation Oscillations and Applications*, Springer-Verlag, New York, 1987.
[9] J. K. Hale, *Diffusive coupling, dissipation, and synchronization*, J. Dynam. Differential Equations, 9 (1997), pp. 1–52.
[10] E. M. Izhikevich, *Phase equations for relaxation oscillators*, SIAM J. Appl. Math., 60 (2000), pp. 1789–1804.
[11] D. Johnston and S. M.-S. Wu, *Foundations of Cellular Neurophysiology*, MIT Press, Cambridge, MA, 1995.
[12] N. Kopell and G. B. Ermentrout, *Symmetry and phaselocking in chains of weakly coupled oscillators*, Comm. Pure Appl. Math., 39 (1986), pp. 623–660.
[13] N. Kopell and G. B. Ermentrout, *Mechanisms of phase-locking and frequency control in pairs of coupled neural oscillators*, in Handbook on Dynamical Systems, Vol. 3: Towards Applications, B. Fiedler, G. Ioos, and N. Kopell, eds., Elsevier, Amsterdam, to appear.
[14] E. F. Mischenko and N. Kh. Rozov, *Differential Equations with Small Parameters and Relaxation Oscillations*, Plenum Press, New York, 1980.
[15] P. F. Pinsky and J. Rinzel, *Intrinsic and network rhythmogenesis in a reduced Traub model for CA3 neurons*, J. Comp. Neurosci., 1 (1994), pp. 39–60.
[16] W. Rall and H. Agmon-Snir, *Cable theory for dendritic neurons*, in Methods in Neuronal Modeling: From Synapses to Networks, C. Koch and I. Segev, eds., MIT Press, Cambridge, MA, 1989, pp. 9–62.
[17] R. H. Rand and P. J. Holmes, *Bifurcations of periodic motions in two weakly coupled van der Pol oscillators*, Internat. J. Non-Linear Mech., 15 (1980), pp. 387–399.
[18] J. Rinzel and G. B. Ermentrout, *Analysis of neural excitability and oscillations*, in Methods in Neuronal Modeling: From Synapses to Networks, C. Koch and I. Segev, eds., MIT Press, Cambridge, MA, 1989, pp. 135–170.
[19] J. Rubin and D. Terman, *Geometric analysis of population rhythms in synaptically coupled neuronal networks*, Neural Comp., 12 (2000), pp. 597–645.
[20] A. A. Samarskii, *Theory of Finite-Difference Schemes*, Nauka, Moscow, 1989 (in Russian).
[21] I. Segev, J. W. Fleshman, and R. E. Burke, *Compartmental models of complex neurons*, in Methods in Neuronal Modeling: From Synapses to Networks, C. Koch and I. Segev, eds., MIT Press, Cambridge, MA, 1989, pp. 63–96.
[22] G .E. Shilov, *Linear Algebra*, Dover Publications, New York, 1977.
[23] F. K. Skinner, N. Kopell, and B. Mulloney, *How does the crayfish swimmeret system work?*

Insights from nearest-neighbor coupled oscillator models, J. Comput. Neurosci., 4 (1997), pp. 151–160.

[24] D. Somers and N. Kopell, *Rapid synchronization through fast threshold modulation*, Biol. Cybern., 68 (1993), pp. 393–407.

[25] D. Somers and N. Kopell, *Waves and synchrony in networks of oscillators of relaxation and non-relaxation type*, Phys. D, 89 (1995), pp. 169–183.

[26] D. W. Storti and R. H. Rand, *Dynamics of two strongly coupled relaxation oscillators*, SIAM J. Appl. Math., 46 (1986), pp. 56–67.

[27] D. L. Wang, *Emergent synchrony in locally coupled neural oscillators*, IEEE Trans. Neural Networks, 6 (1995), pp. 941–948.

[28] X. J. Wang and J. Rinzel, *Oscillatory and bursting properties of neurons*, in Handbook of Brain Theory and Neural Networks, M. A. Arbib, ed., MIT Press, Cambridge, MA, 1995, pp. 686–691.

[29] D. L. Wang and D. Terman, *Global competition and local cooperation in a network of neural oscillators*, Phys. D, 81 (1995), pp. 148–176.

[30] C. J. Wilson and J. C. Callaway, *A coupled oscillator model of the dopaminergic neuron of the substantia nigra*, J. Neurophysiol., 83 (2000), pp. 3084–3100.